NOTICE

The quality of this microform is heavily dependent upon the quality of the original thesis submitted for microfilming. Every effort has been made to ensure the highest quality of reproduction possible.

If pages are missing, contact the university which granted the degree.

Some pages may have indistinct print especially if the original pages were typed with a poor typewriter ribbon or if the university sent us an inferior photocopy.

Reproduction in full or in part of this microform is governed by the Canadian Copyright Act, R.S.C. 1970, c. C-30, and subsequent amendments.

AVIS

La qualité de cette microforme dépend grandement de la qualité de la thèse soumise au microfilmage. Nous avons tout fait pour assurer une qualité supérieure de reproduction.

S'il manque des pages, veuillez communiquer avec l'université qui a conféré le grade.

La qualité d'impression de certaines pages peut laisser à désirer, surtout si les pages originales ont été dactylographiées à l'aide d'un ruban usé ou si l'université nous a fait parvenir une photocopie de qualité inférieure.

La reproduction, même partielle, de cette microforme est soumise à la Loi canadienne sur le droit d'auteur, SRC 1970, c. C-30, et ses amendements subséquents.

Visualization of Water/Oil Displacement in Porous Media in the Presence of Chemical Reaction

by

Masoud Gholamhosseini

A thesis submitted to
the school of Graduate Studies
in partial fulfillment of the requirements for the
degree of Master of Applied Science
in
Chemical Engineering

DEPARTMENT OF CHEMICAL ENGINEERING
UNIVERSITY OF OTTAWA
OTTAWA. ONTARIO,

ISBN 0-315-75078-2

UNIVERSITÉ D'OTTAWA
UNIVERSITY OF OTTAWA

dedicated to my family

ABSTRACT

In enhanced oil recovery, low interfacial tension, optimum wettability condition, high pH value, and the electric charge density at the interface can improve the oil recovery percentage appreciably. However, the addition of sodium hydroxide changes the interfacial tension to an ultra-low value. Interfacial tension decreases as a result of the interfacial reaction between the surface active species in the oleic phase and the caustic in the aqueous phase. The surface active species also provide favorable wettability conditions and interfacial activity which improves the recovery percentage.

This study has investigated the effects of caustic concentration in the aqueous phase on the recovery percentage, and on the displacement pattern in a radial cell. The caustic solutions were employed as the displacing phase being brought into contact with the acidic oil in the cell. The displacing aqueous phase contained different concentrations of sodium hydroxide ranging from 0.0 mM to 25 mM, and the displaced phase was a light paraffin oil containing 10 mM linoleic acid.

In this research, the effect of flowrate on oil recovery percentage was also examined. The flowrate was varied within the range 0.78 ml/h to 26.8 ml/h, which covered all of the three flow regions (i.e. capillary, intermediate, and the viscous region).

The experimental results show that at a sodium hydroxide concentration of 25 mM higher recovery percentages were obtained than at other sodium hydroxide concentrations, and that the flowrate was inversely proportional to the recovery percentage. The highest recovery percentage was obtained at the lowest working flowrate (i.e. 0.78 ml/h), with a caustic concentration of 25 mM.

In the capillary region, where the flowrates were low, by increasing the pH the recovery percentages were similarly increased for the complete spectrum of sodium

hydroxide concentrations.

In the viscous region, where the flowrates were high, the recovery percentages were not sensitive to either the flowrate, or to the sodium hydroxide concentration.

ACKNOWLEDGEMENTS

Special appreciation is expressed to Drs. G. Neale and V. Hornof for their assistance, guidance, and supervision during this project. The dedicated efforts of Messrs G. Gasperetti, L. Tremblay, and A. Bonaldo in the Departmental Machine Shop are also gratefully acknowledged.

Contents

List of Tables

List of Figures

Notation

Various symbols, superscripts, subscripts, accents and abbreviations used frequently in this work are summarized below. All notation is fully defined where it first arises in the text.

Symbols

A^-	surface active species.
$C_{A^-_s}$	sublayer concentration of A^-, $[mole.m^{-3}]$.
c	molar concentration.
D	diffusion coefficient, $[cm^2.s^{-1}]$.
HA_o	acid in oleic phase.
HA_w	acid in aqueous phase.
h	thickness of the cell, $[cm]$.
K	permeability, $[\mu m^2]$.
K_1	absorption rate constant, $[m.s^{-1}]$.
K_2	desorption rate constant, $[s^{-1}]$.
M	mass, $[g]$.

N_{ca} capillary number.

n_A adsorbed mole of A per unit area, $[mole.m^{-2}]$.

n_{A^-} adsorbed mole of A^- per unit area ,$[mole.m^{-2}]$.

n_{max} maximum adsorbed mole per unit area, $[mole.m^{-2}]$.

P pressure, $[mN.m^{-2}]$.

Q flowrate, $[ml.h^{-1}]$.

r radius of the finger, $[cm]$

R gas constant, $[J.mole^{-1}.K^{-1}]$, radius of the cell, $[cm]$

R_1 first breakthrough radius, $[cm]$.

R_2 second breakthrough radius, $[cm]$.

R_3 third breakthrough radius, $[cm]$.

t time, $[s]$.

t_{br} breakthrough time, $[s]$

T absolute temperature, $[K]$.

v molar volume.

V total volume, $[cm^3]$, velocity, $[cm.s^{-1}]$.

S spreading coefficient, $[mN.m^{-1}]$.

U velocity, $[cm.s^{-1}]$.

$W_{o/w}$ work of cohesion, $[mN.m^{-1}]$.

$W_{o/o}$ work of adhesion, $[mN.m^{-1}]$.

Superscripts

l	liquid phase.
o	oleic phase.
w	aqueous phase.
s	solid, surface.

Abbreviations

IFT	interfacial tension.
SDT	spinning drop tensiometer.
Rec	recovery.

Greek letters

ρ	The molar density, $[kg.m^{-3}]$.
γ_i	interfacial tension, $[mN.m^{-1}]$.
γ_o	surface tension, $[mN.m^{-1}]$.
θ	contact angle.
μ	viscosity, $[mPa.s]$.
Ψ_0	interfacial potential, $[volt]$.
ε	porosity.

Chapter 1

Introduction

1.1 History of Alkaline Flooding

The first attempt to forcefully recover oil was made in Sweden prior to 1740 [1]. The Swedish engineers used the water-flooding method to recover oil, however, they soon realized that the effectiveness of the method is affected by such complications as surface forces, and gas bubbles in the reservoir. Both of these factors cause oil entrapment in the reservoir.

Since then, enormous efforts have been made to reduce interfacial tension (IFT) and to change wettability conditions in the reservoir. This explains why relatively inexpensive alkali is added to the water during the flooding method. Specifically, addition of caustic to water-flooding alters the oil-water-rock contact angle, and as a result the extent of surface forces (which entrap the oil during the displacement process) changes. In 1917 Squires was the first person to initiate the addition of

caustic to water-flooding to improve the recovery percentage [1].

1.2 Enhanced Oil Recovery

Research confirms that most crude oils naturally contain acidic components [2,3,4,5]. The alkaline flooding method for enhancing underground crude oil recovery is based on the generation of surfactants in situ. The surfactants are produced in a reaction between acidic components in the oil phase with caustic in the aqueous phase. The surface active anion accumulation at the interface lowers the interfacial tension (IFT) to ultra low values. Therefore, alkaline flooding is one of the most suitable methods for acidic oil recovery.

1.3 Viscous Fingering

When a less viscous fluid displaces a fluid of higher viscosity, the less viscous fluid has a tendency to finger through the more viscous fluid. In the absence of gravity forces (for example in horizontal displacement), viscosity differences between the displacing phase and the displaced phase cause the fingering phenomenon. If the viscosities of the two phases are equal, the difference in the saturation of the two phases causes the fingering of one phase through the other. The fingers pass through the path of least hydrodynamic resistance. Fast growing fingers result in premature breakthrough, and this leads to a lower recovery percentage.

Some of the methods can be used in enhanced oil recovery to improve recovery percentage are as follows: (1) water flooding; (2) CO_2 injection; (3) in situ combustion; (4) alkaline flooding; and (5) polymer injection.

Among above mentioned methods, alkaline flooding can be used to dampen the growth of fast growing fingers (i.e. premature breakthrough time t_{br}):

1.4 Objectives of This Study

The principal objective of this study was to determine the effects of sodium hydroxide concentration and pH on recovery percentage of oil from a consolidated porous medium. A radial displacement geometry, similar to that found in a real oil well, was employed.

A secondary objective was to explore the effects of the injection flowrate on the displacement patterns and the breakthrough recovery times in the cell.

Chapter 2

Theory

2.1 Alkaline Flooding and IFT

2.1.1 Dynamic IFT Behavior of Caustic Solutions when Displacing Acidic Oil

Many researchers [6,7,8,9] have studied IFT behavior of alkaline solution in contact with acidic oil in a batch system. However, there remain unexplained many characteristics about the mechanism of dynamic IFT behavior of alkaline solutions when displacing acidic oils in the cell.

In the visualization of two immiscible fluids, when one fluid displaces another one in the presence of chemical reactions in the cell, the researcher is faced with complicated problems. Some of these difficulties are:

(1) the volume ratio of the two phases (displacing and displaced phases) is time

dependent, i.e. it is not constant.

(2) chemical reactions between the acid in the oil phase with the sodium hydroxide in the aqueous phase (see equation (2.1) occur in the large three dimensional surface areas (see Fig. 2.1).

$$R - COOH + NaOH \rightleftharpoons R - COONa + H_2O \tag{2.1}$$

This means that the interface of the displacing phase with the displaced phase is not a simple two dimensional surface area such as represented by Fig. 2.2. Three dimensional surface areas are more complicated to analyze than two dimensional surface areas.

(3) since the mobility ratio of the displacing phase to the displaced phase is greater than one (for example 20.16), there is viscous fingering and convective diffusion at the interface. This type of diffusion is not the simple Fickian type. Sharma et al. [10] suggest that the sequence of events (diffusive convection, chemical reaction, diffusive convection) gives rise to interesting maxima and minima of IFT as dictated by the relative kinetics of each step.

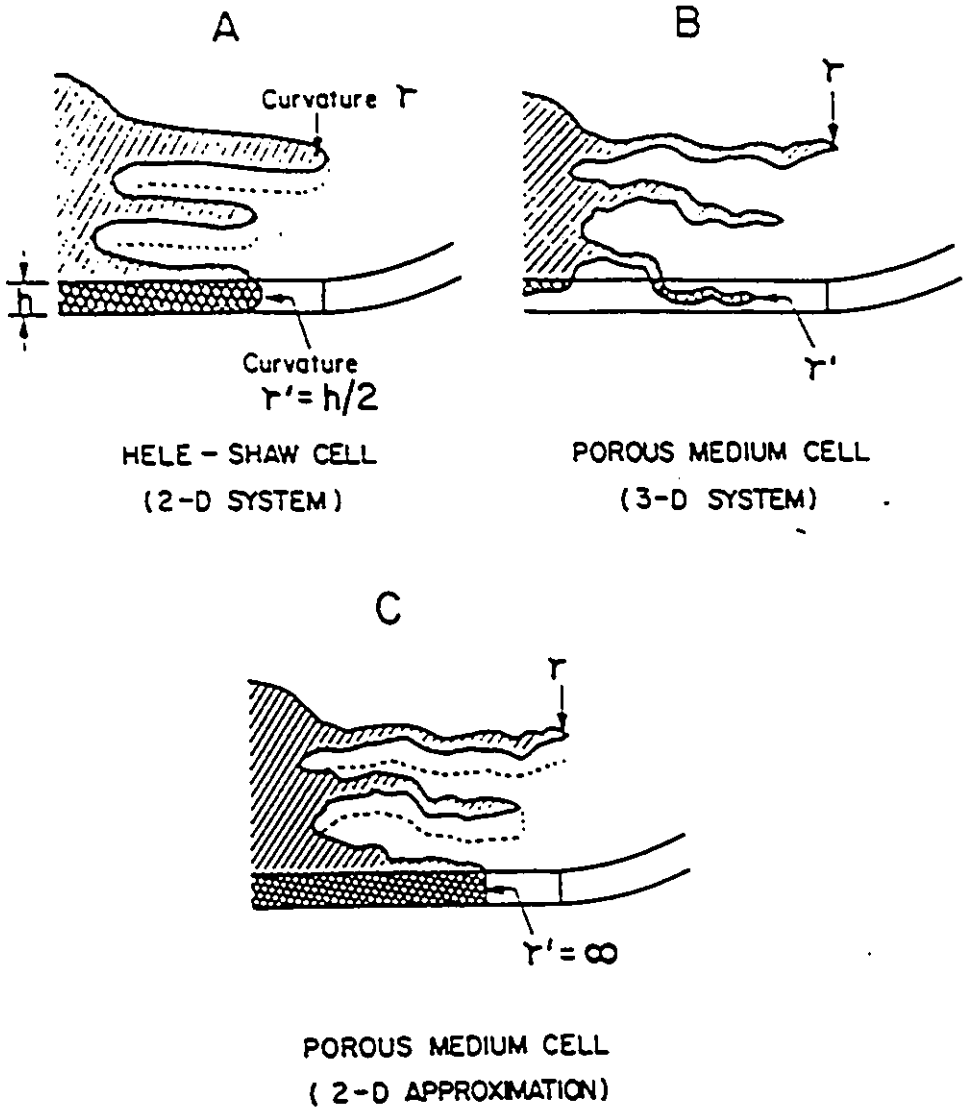

Figure 2.1: Three-dimensional interface of two immiscible phases in a porous medium cell (hatched zone).

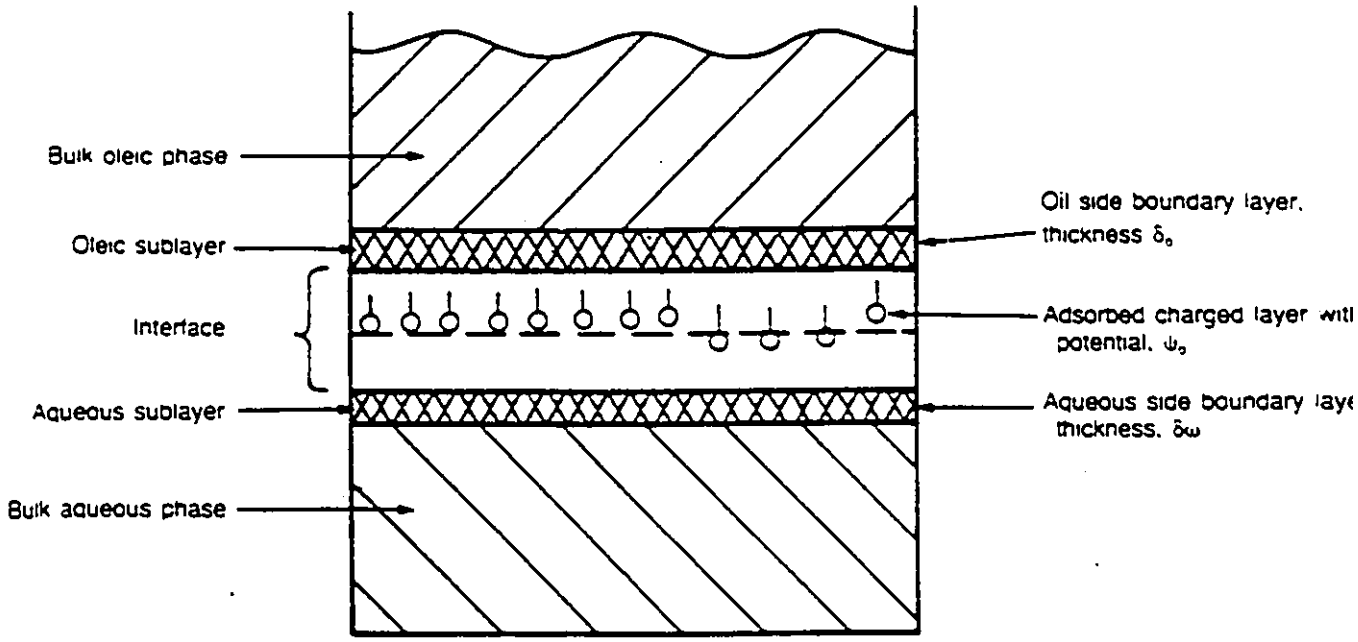

Figure 2.2: Two-dimensional interface of two immiscible phases in a porous medium cell (using the Gibbs model of the interface).

(4) mass transfer, adsorption, and desorption

- mass transfer of both chemical reactants from the bulk phase to the interface and vice versa.

- adsorption and desorption of surface active species to and from the interface (surface active species are produced as a consequence of interfacial reaction between the acid in the displacing phase and sodium hydroxide in the displaced phase).

(5) the minimum and maximum IFTs measured with the Spinning Drop Tensiometer(SDT) vary widely from the minimum and maximum IFTs that occur inside the cell where the two phases come into contact with each other.

All of the above problems make it very difficult to perform a reliable quantative analysis of the dynamic IFT behavior inside the cell, where the displacing phase comes into contact with the displaced phase. It is also difficult to derive an approximate governing equation of mass transfer of surface active species from the bulk phases to the interface and vice versa which is a consequence of convective diffusion of those species in the porous medium.

Hence, the researcher requires at least an approximate theoretical analysis of dynamic IFT behavior between the acidic oil and the alkaline solution in the cell, together with a qualitative analysis of the most suitable wettability conditions.

2.2 Mass Transfer Mechanism

2.2.1 Alkaline Flooding and Mass Transfer of Surface Active Species

Research has established that surface active species in alkaline flooding lower the IFT values markedly. Surface active species are produced as a consequence of interfacial reactions between the acid in the oleic phase and the caustic in the aqueous phase. These reactions lead to formation of surfactants in situ. DeZabala et al. [11] stated that one thing which distinguishes alkaline flooding from other methods is its ability to produce surfactant in situ .

England and Berg [12] suggested a Fickian diffusion model to describe the transfer of surface active agents across a liquid-liquid interface and the presence of an activation barrier to adsorb and/or desorb the chemical reactants. In alkaline studies the individual should know that convective-diffusion of surface active species from the bulk phase to the interface and vice versa exists and is not of the simple Fickian diffusion.

Rubin and Radke [13] suggested the transfer of solute from one liquid phase through the interfacial region may be conceptualized in the following steps:

(1) convective diffusion from the bulk phases to the interface; (2) adsorption into the interface; (3) reaction at the interface; (4) desorption from the interface;

and (5) convective diffusion into the second bulk phase.

The above sequence of events determines the time evolution of the boundary tension.

2.2.2 Surface Active Species and Convective Diffusion

It is well established that diffusion of material from the oleic phase to the aqueous phase and vice versa occurs to the following sequence of events:
i) the acid in the oil diffuses to the aqueous phase. The distribution of the acid between the oleic and the aqueous phases is given by the following equation :

$$HA_o \rightleftharpoons HA_w \tag{2.2}$$

ii) the acid that is absorbed by the aqueous phase is dissociated to form hydronium ions and the surface-active species A^-. Thus:

$$HA_w + H_2O \rightleftharpoons H_3O^+ + A^- \tag{2.3}$$

iii) the formation of inactive soap (NaA), as follows:

$$Na^+ + A^- \rightleftharpoons NaA_w \tag{2.4}$$

Rubin and Radke [13] formulated a theory of dynamic IFT minima by postulating the presence of a diffusion boundary layer and using the Nernst film model to calculate the rate of convective diffusion of solute.

Eq. 2.1 shows the reaction between linoleic acid and sodium hydroxide.

2.2.3 Adsorption and Desorption of Active Species

Ramakrishnan and Wasan [14] used Gouy-Chapman's theory of the diffuse double layer to model the adsorption and desorption of active species at the interface. Ramakrishnan and Wasan [14] also related the IFT reduction to the concentration of the surface active species using Gibbs's equation. Finally, the adsorption kinetic term (the first term in equation 2.4) of the A^- surfactant was suggested by Ramakrishnan and Wasan [14]. Guastalla [15] suggested the desorption kinetic term(second term in equation 2.4) of surfactant A^-, thus:

$$\frac{dn_{A^-}}{dt} = K_1 C_{A_s^-}\left(1 - \frac{n_{A^-}}{n_{max}}\right) - K_2 n_{A^-} \exp\left(-\frac{W}{RT}\right) \tag{2.5}$$

2.2.4 Effect of pH on Surface Active Species

Sharma et al. [10] have discussed the dissociation of acid species. The extent of dissociation is governed by the pH of the surface phase.

In agreement with the work of Sharma et al. [10], deZabala et al. [11] stated that the acid dissociation constant controls the pH range as expected in surfactant hydrolysis, (equation 2.6).

$$HA_w \rightleftharpoons H^+ + A^- \tag{2.6}$$

Chan and Yen [16] mentioned that the activation reaction is the dissociator of the acid at alkaline pHs. This generates the interfacially active species A^-. Trujillo [17] presented a mass-action relationship that described the equilibrium IFT at a constant ionic strength between crude oils and sodium hydroxide solutions as a function of pH.

2.3 Alkaline Flooding and Wettability

2.3.1 Some Basic Concepts in Enhanced Oil Recovery

Surface Tension

Consider a drop of one component liquid in equilibrium with its vapor in the absence of any external force (for example gravity). Since the free surface energy of a system tends to a minimum value, the surface area of a pure phase will tend to decrease spontaneously (i.e. the surface will contract spontaneously).

Fig. 2.3(a) shows that asymmetrical forces at the surface cause the liquid to contract at the surface spontaneously; therefore, one can imagine a liquid surface to be in state of tension. The force per unit length that contracts a liquid surface is called the *surface tension* (γ_o). In other words, surface tension is a direct measure of the contractile tendency of a liquid surface.

Since force components are distributed asymmetrically at the surface, the free energy of the surface molecules is greater than that of the interior molecules. This free energy is called *excess free energy* which is not the total free energy of the system.

Interfacial Tension

If a liquid is placed in contact with another liquid, the interface between the two liquids also has contractile tendency. This is called *interfacial tension* (IFT) represented as γ_i (mN/m). For example the IFT between water and butanol (partially miscible in water) is 1.8 (mN/m), since the molecules of butanol concentrate at the oil-water interface, thereby decreasing the usual contractile tendency of the interface. This phenomena results in an IFT reduction between water and butanol. The interfacial orientation of butanol is favored since the hydrocarbon chain is hydrophobic, see Fig. 2.3(b).

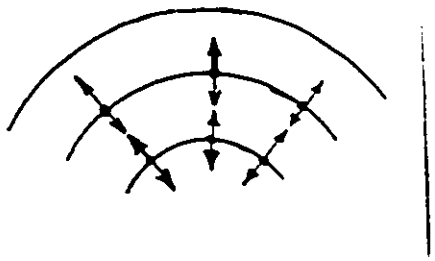

(a)

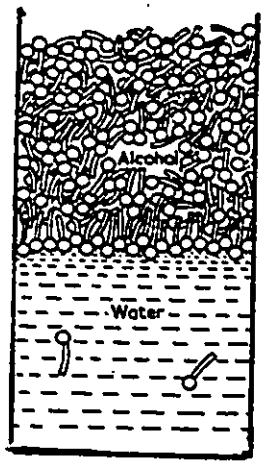

(b)

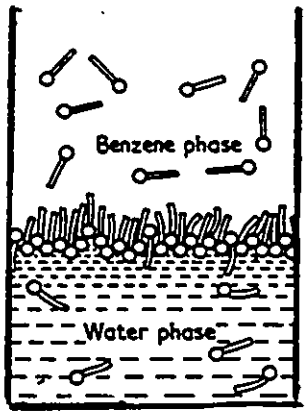

(c)

Figure 2.3: (a): Surface tension as a result of asymmetrical surface forces (b): Interfacial tension between butanol and water as a result of contractile tendency of interface. (c): Reduction of the interfacial tension between benzene and water as a result of the presence of third component (butanol).

Spreading Pressure

Adding a third component such as butanol (partially miscible in oil) to a two component system of oil/water causes excessive repulsive forces at the oil/water interface. The repulsive force tends to decrease the contractile tendency of the interface, thereby decreasing γ_i. This excessive repulsion force at the interface is called the *spreading pressure*, see Fig. 2.3(c).

Work of Adhesion and Cohesion

The amount of work required to separate the interface of two liquids is called the work of *cohesion*. However it is called the work of *adhesion* when the two liquids are the same. Cohesion work ($W_{o/w}$) and adhesion work ($W_{o/o}$) are presented in terms of interfacial tension in the following equations:

$$W_{o/w} = \gamma_{o/a} + \gamma_{w/a} - \gamma_{o/w} \tag{2.7}$$

where $\gamma_{o/a}$, $\gamma_{w/a}$, and $\gamma_{o/w}$ are the interfacial tensions between oil and air, water and air, and oil and water, respectively.

Work of adhesion was formulated as follow:

$$W_{o/o} = \gamma_{o/a} + \gamma_{o/a} - \gamma_{o/o} \tag{2.8}$$

Since $\gamma_{o/o}$ is always zero Equation 2.7 reduces to : 2.8.

$$W_{o/o} = 2\gamma_{o/a} \tag{2.9}$$

2.3.2 Spreading Coefficient

When a liquid is spread on another liquid, the *spreading coefficient* equation of liquids [18] is defined as follows:

$$S_{o/w} = \gamma_{w/a} - \gamma_{o/a} - \gamma_{o/w} \tag{2.10}$$

or

$$S_{o/w} = W_{o/w} - W_{o/o} \tag{2.11}$$

(1) spreading occurs when $W_{o/w} > W_{o/o}$

(2) spreading never occurs if either $W_{o/w} < W_{o/o}$ or $\gamma_{o/a} > \gamma_{w/a}$.

2.3.3 Contact Angle

As shown in Fig. 2.4 (a), the angle θ between the solid and the oil/water interface is defined as the contact angle. The contact angle reflects wetting in a following manner:

(1) if $\theta = 0$, there is complete wetting of the solid

(2) if $\theta = \pi$, there is complete non-wetting of the solid

(3) if $0 < \theta < \pi$, there is incomplete wetting of the solid

Equation 2.11 satisfies the interfacial tensions components between air, liquid, and solid in Fig. 2.4(a). Equation 2.11 was formulated by Cockbain and Schulman [19].

$$\gamma_{s/a} = \gamma_{s/l} + \gamma_{l/a} \cos\theta \tag{2.12}$$

For this system, the work of adhesion is

$$W_{s/l} = \gamma_{s/a} + \gamma_{l/a} - \gamma_{s/l} \tag{2.13}$$

Combining equations 2.11 and 2.12 yields:

$$W_{s/l} = \gamma_{l/a}(1 + \cos\theta) \tag{2.14}$$

2.3.4 Water-Wet and Oil-Wet Systems

Bartell [20] stated that solids may be divided into two classes; hydrophilic solids which, are wet more rapidly by water than by organic liquids (these solids are called water-wet); and hydrophobic solids which are wet more rapidly by organic liquid than by water (these solids are known as oil-wet solids).

Fig. 2.4(b) is a water-wet system because it is preferentially wet by water without application of any external forces. Generally, this phenomenon is known as capillary imbibition.

Fig. 2.4(c) shows a system that is preferentially wet by oil; therefore it is termed an oil-wet system.

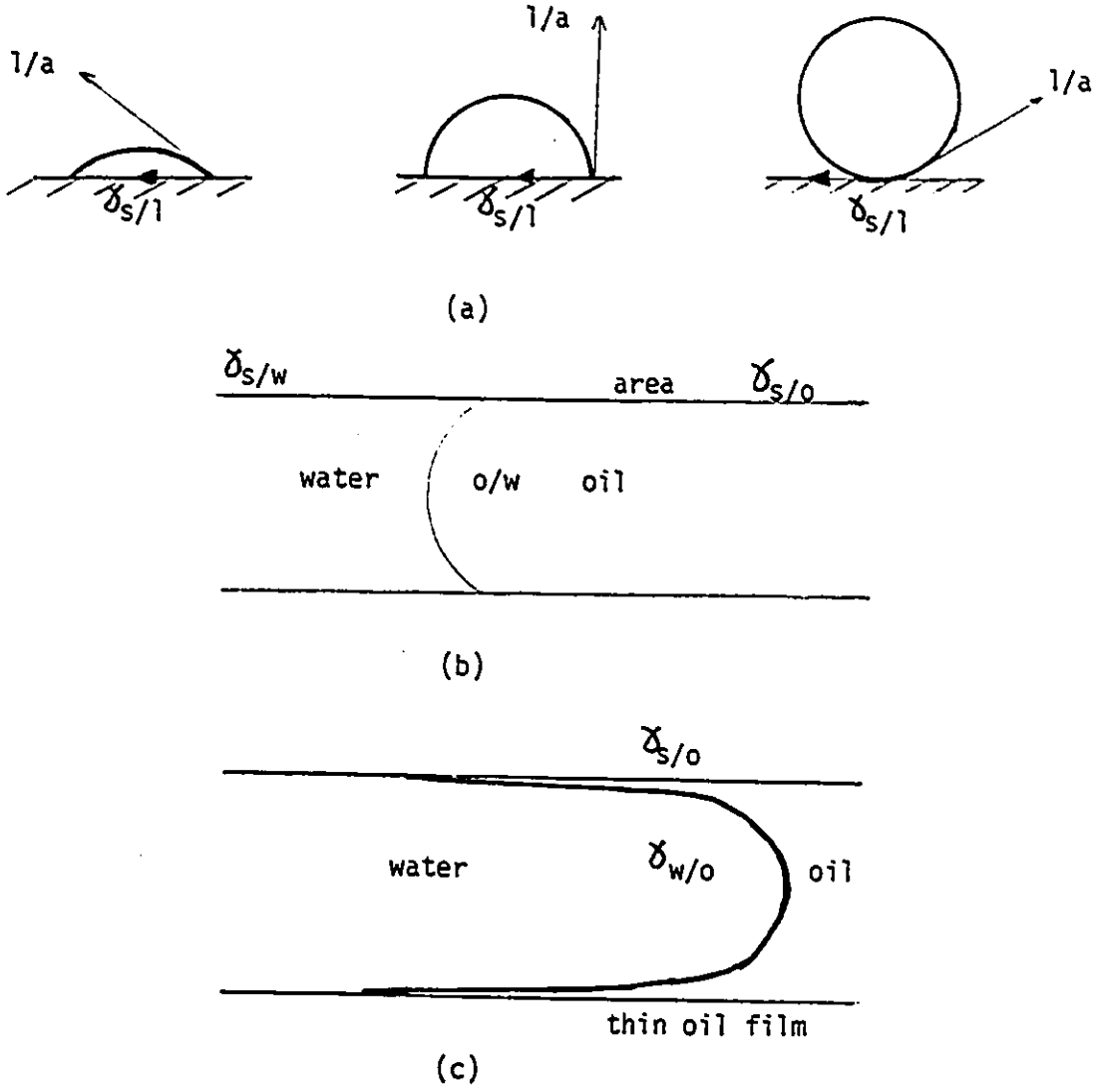

Figure 2.4: (a): Contact angle between Solid/Oil/Water (b): Water wet system in a capillary tube (c): Oil wet system in a capillary tube

In practical light oil recovery processes, water-wet systems generally yields higher recovery percentages than do $oil - wet$ systems.

2.3.5 Wettability Alteration

Wettability alteration is one of the most important characteristics of alkaline flooding. Morrow [21] stated that reservoir wettability is determined by complicated interfacial boundary conditions acting within the pore space of the reservoir rock. These conditions have a dominant effect on interface movement and associated oil displacement. Cook et al. [22] proposed that wettability alteration plus IFT reduction was a factor in oil recovery with caustic.

2.3.6 Contact Angle and Adhesion

Contact angle is the most universal measure of surface wettability, see Fig. 2.4(a). Wetting properties of a solid are dominated by the outermost layer of molecules. Large changes in surface wettability can be achieved by the adsorption of a monolayer of polar molecules so that the outermost layer of the surface is composed of a hydrocarbon chain.

Adhesion and cohesion behavior of an oil/brine/solid system causes increasing or decreasing contact angles. This behavior produces different surface wettability

conditions.

Bartell [20] showed that both advancing and receding contact angles have important effects on oil recovery. Because of the very complex nature of the surface forces involved, it is difficult to obtain a reliable evaluation of the effect of wettability on the oil recovery percentage. Even more difficult is the study of contact angle in porous media.

The addition of alkali to an aqueous phase was initiated by Squires in 1917. In 1956, Reisberg and Doscher [23] showed that the acidic oils could be easily removed from glass surfaces by adding alkali to the aqueous phase. Wagner and Leach [24] showed that drastic wettability alteration of the reservoir occurs during high pH alkaline flooding which in turn changes the contact angle of the system.

In practice, optimum recovery percentage generally occurs at the most suitable wettability condition.

2.4 Charge Density and Alkaline Flooding

2.4.1 Interfacial Potential

When an oleic phase containing a fatty acid (such as linoleic acid) comes into contact with an aqueous phase containing a base (such as sodium hydroxide), a potential difference (Ψ_0) is established at the interface of the two phases. This

interfacial potential difference (Ψ_0) is the result of an unequal distribution of the various anions and cations across the interface. This causes the phases on each side of the interface to become electrically charged.

Davis and Rideal [25] stated that the presence of an electric charge on a monolayer greatly alters its properties and, in particular, if a fatty acid film becomes ionized by formation of its soap, there is a great diminution of the net lateral adhesion between film- forming molecules.

2.4.2 Effect of Interfacial Potential on Interfacial Tension and pH

Bansal [26] stated that the lowest IFT between caustic solution and crude oil occurs at the highest negatively charged interface. Cratin [27] explained the dependence of IFT on pH. Cratin [27] showed that at high pH's asphaltene become negatively charged and are more negatively charged. This leads to a lower IFT value.

Ramakrishnan and Wasan [14] proposed a model to calculate interfacial potential. This model shows a fair agreement with the electrophoretic mobility (the ratio of electric field strength to velocity of particles) measurements. Shah et al. [28] observed that as the electrophoretic mobility of the oil droplets change so does IFT, proposing that the excess sodium hydroxide increases IFT perhaps by decreasing

the interfacial charge density.

Chan and Yen [29] discussed the effect of pH on IFT, they stated that the sudden IFT drop between acidic oil and alkaline solution corresponds to the ionization of the $R-COOH$ acid species to the active $R-COO^-$ species at high pH.

2.5 Capillary Number

The ratio of the viscous to the capillary forces is defined as the capillary number (Eq. 2.15) which is a dimensionless number in enhanced oil recovery.

$$N_{ca} = \frac{\mu V}{\varepsilon \gamma} \tag{2.15}$$

where μ is the viscosity of the displacing phase, ε is porosity of porous medium, γ is the interfacial tension between the displacing and the displaced phases, and V is the superficial velocity of the circular front of the displacing phase which is defined as follows for radial displacement geometry :

$$V = \frac{Q}{2\pi r h} \tag{2.16}$$

where Q is the volumetric flowrate, r is the radius of the circular front of the displacing phase, and h is the thickness of the layer between the two circular plates.

Equation 2.16 shows that for a given flowrate, V is a function of the radius of the circular front of the displacing phase and so is the capillary number.

The recovery versus flowrate curve can be divided into three regions (Fig. 4.9), as follows :

(1) the capillary region, where the capillary number is lower than those in the intermediate and the viscous regions; (2) the viscous region, where the capillary number is higher than those in the intermediate and the capillary regions: and (3) the intermediate region where, the capillary number lies between those of the capillary and the viscous regions.

Table 2.1 shows the capillary number for the three different regions at the cell exit.

Table 2.1: Division of three regions in terms of capillary number

Name of the region	Capillary number
Capillary	$< 7.9 \times 10^{-7}$
Intermediate	5.5×10^{-6}
Viscous region	$> 6.8 \times 10^{-5}$

Chapter 3

Experimental Studies

3.1 Experimental Design

3.1.1 Elements of a Working System

Displacing and Displaced Phase

Based on previous works [30,31,32,33] ,light paraffin oil with 10 mM linoleic acid was selected as the displaced phase (oleic phase) and for the reasons mentioned in section 1.1 and 1.2, sodium hydroxide (NaOH) was used as the caustic reagent in the aqueous phase (displacing phase).

The Radial Cell

The displacement experiments were conducted in a model consolidated porous medium.

In practical enhanced oil recovery (EOR), one source injection point is normally used. That was the rationale for experimenting with a radial cell (radial displacement), instead of using a rectangular cell which has multi-injection source points (linear displacement).

3.1.2 Properties and Manufacturing of the Cell

Table 3.1 gives the specification of the two cells used in this work:

Table 3.1: Properties and manufacturing of the cell

Cell No.	Porosity	Permeability	Thickness	Cell Radius	Glass beads size
	ε	K(μm^2)	h (cm)	R (cm)	Mesh
I	0.39	72	0.3	7.9	42-48
II	0.58	62	0.3	7.9	36-42

The porous medium consisted of sintered spherical glass beads that are sandwiched between two parallel circular glass plates (see Fig. 3.1).

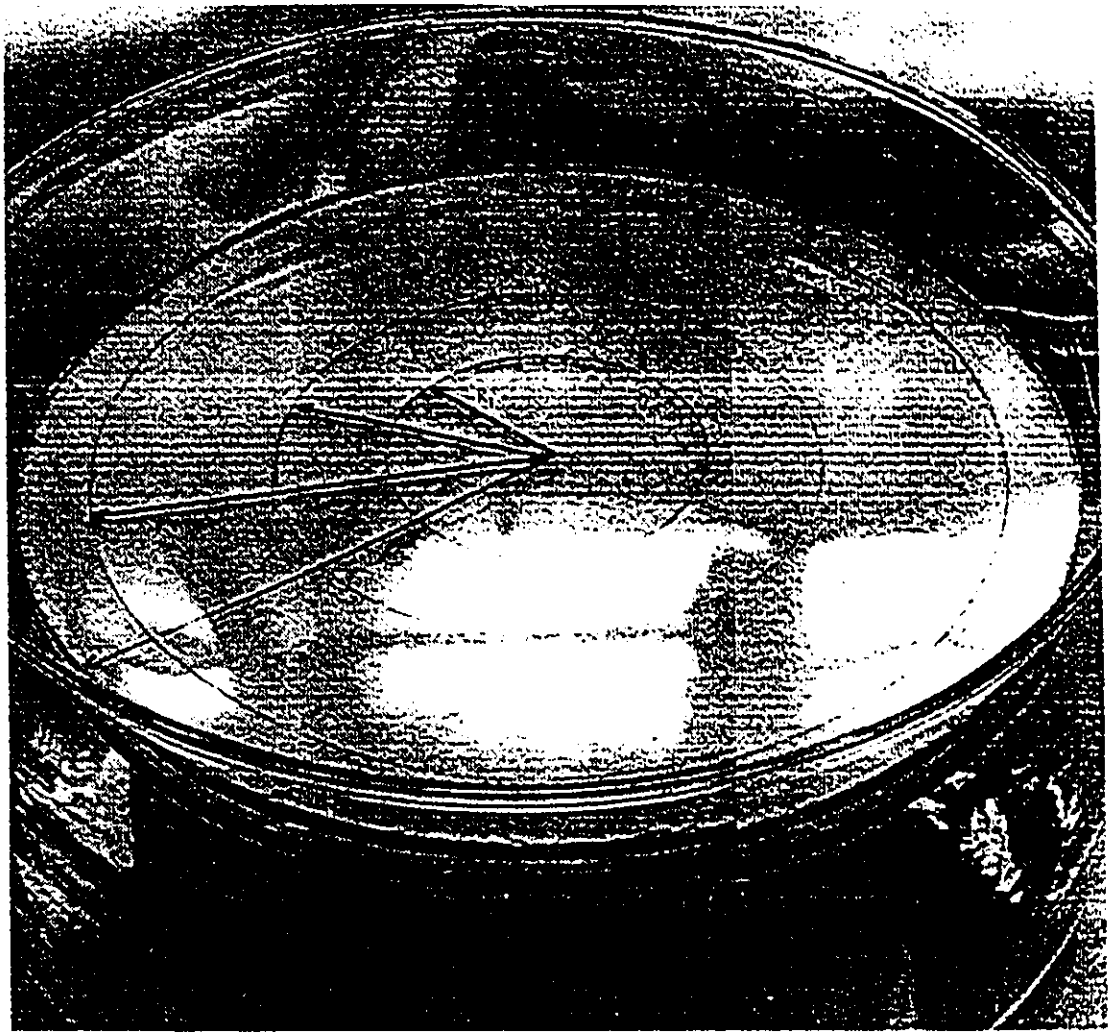

Figure 3.1: Sintered glass beads sandwiched between two circular plates. Radial Cell

3.2 Cell Characteristics

Each cell has its own characteristics, such as porosity, permeability, homogeneity, and wettability. Before starting the experiments the porosity and permeability of the cell were initially measured, and the wettability and homogeneity of the cell were checked.

This study discusses the visualization of caustic/acidic oil displacements. Since the visualization of displacement of one phase by another phase in unconsolidated porous media is not reproducible with respect to parameters such as porosity, wettability, and structural heterogeneity [5], this study examined a consolidated porous medium.

3.2.1 Porosity

To determine the porosity of the cell, two circular glass plates were weighed (M_{plates}) before the cell was manufactured. After the sintered glass beads were sandwiched between two glass plates under a 560°C temperature, the cell was also weighed (M_{cell}). Pore volume (V_{pore}) and porosity (ϵ)were obtained with the following calculations:

$$V_{glass-beads} = \frac{M_{cell} - M_{plates}}{\rho_{glass-beads}} \tag{3.1}$$

$$V = \pi R^2 h \tag{3.2}$$

where V is the volume of the cell, h is the thickness of the layer between the two plates, and R is the radius of the cell.

$$V_{pore} = V - V_{glass-beads} \tag{3.3}$$

Porosity is easily obtained by equation 3.4:

$$\varepsilon = \frac{V_{pore}}{V} \times 100 \tag{3.4}$$

3.2.2 Permeability

Fig. 3.2 shows the experimental set-up that was used to determine permeability (μ) using equation 3.5:

$$K = \frac{{R_1}^2 \mu}{2t\omega\rho g} \ln\frac{R_2}{R_1} \ln\frac{h_1}{h_2} \tag{3.5}$$

where $h_1 > h_2$.

Table 3.2 gives the experimental data that was used to calculate the average permeability.

Table 3.2: The experimental data to calculate the average permeability

ω	h(t)	t	Δt	permeability
cm	cm	seconds	seconds	μm^2
35.5	5.5	0		
35	6	44	44	79.72
34	7	154	110	65.17
33	8	258	104	70.9
32	9	367	109	69.8
31	10	480	113	69.4
30	11	605	115	70.5
29	12	722	117	71.6
28	13	847	125	69.41
27	14	970	123	73.12
26	15	1100	130	71.79
25	16	1238	138	70.2
24	17	1375	137	70.5
23	18	1518	143	73.6
22	19	1660	142	77.4
21.1	19.9	1815	155	00000

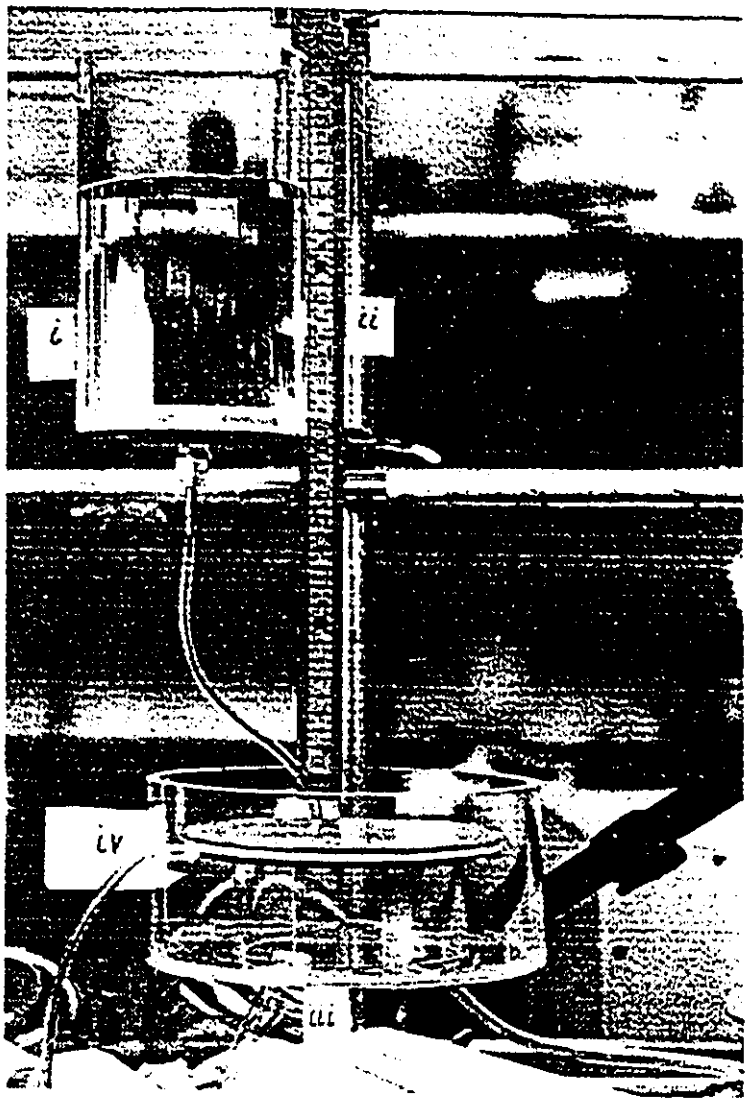

Figure 3.2: Permeability experimental set-up: i: water vessel; ii: ruler to measure height of water; iii: saturated cell with water; iv: water dish

3.2.3 Wettability

The porous medium was shown to be water-wet, since, when the oil-saturated cell was immersed into water, spontaneous imbibition occurred (refer to section 2.3.4 discusses water-wet system). All of experiments in this study were done in a water-wet porous medium.

3.2.4 Homogeneity

An experiment was implemented to check whether the cell was macroscopically homogeneous or not. In this experiment the displacing phase and the displaced phase were double distilled water. The displacing phase was dyed with food coloring to be distinguished from the displaced phase .

Since the viscosity ratio was unity and the density was the same for both phases, the displacement pattern was observed to be of a circular shape (see Fig. 3.3) This circular displacement pattern established that the cell was homogeneous [34,35].

3.3 Experimental Set-Up

The experimental set-up consisted of the cell, an oil-dish, an overhead camera, some connecting hose, and a constant flowrate syringe pump (see Fig. 3.4).

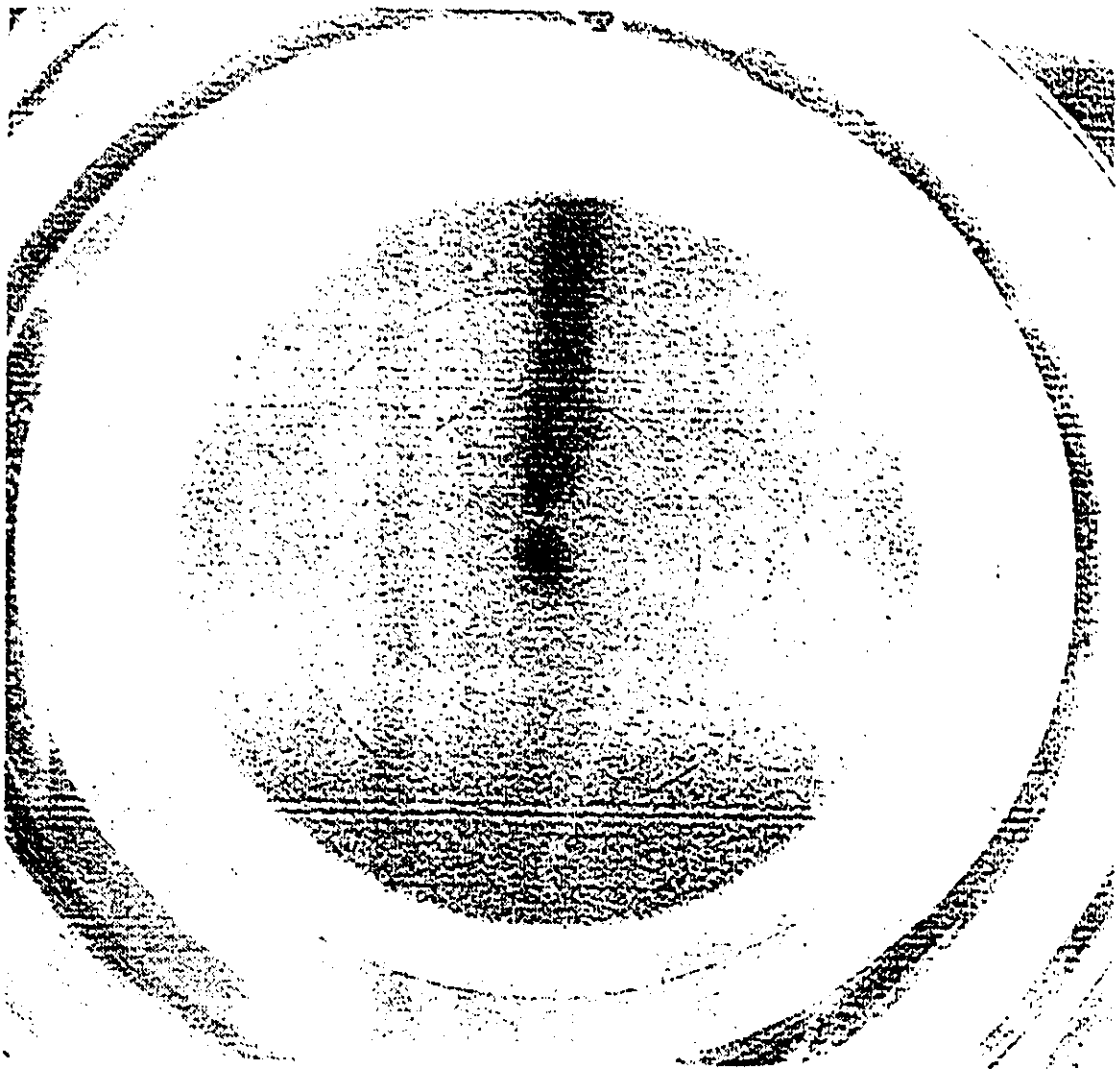

Figure 3.3: Circular displacement pattern shows homogeneous nature of the cell

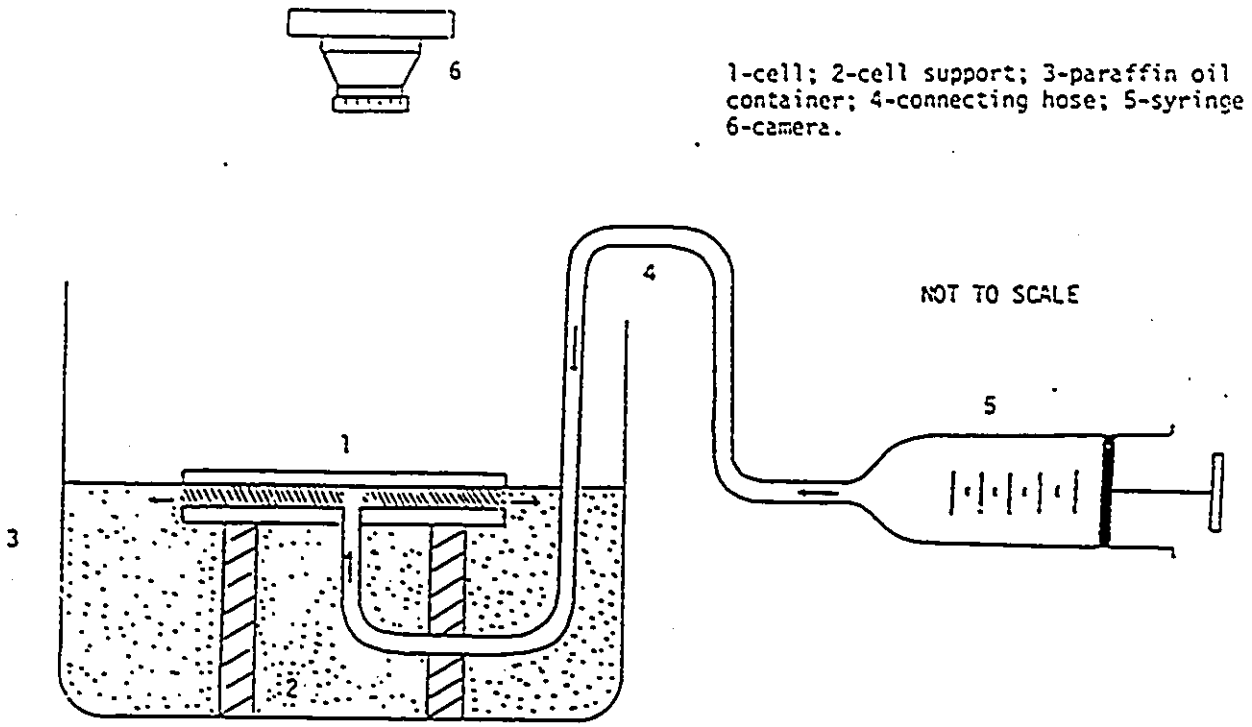

Figure 3.4: Experimental set-up

3.4 Experimental Procedure

To carry out each experiment, these steps was carried out :

(1) the cell was immersed in the oil-dish to achieve cell saturation, the oil saturated cell in the dish was placed under vacuum to remove any air trapped in either the oil saturated cell (Jamin effect) and/or oil in the dish.

(2) the flowrate selector was set to provide an appropriate flowrate, thereby bringing aqueous phase into contact with oleic phase.

(3) for each experiment, a picture was taken at three different radii of the cell (i.e. R_1, R_2, and R_3 , see Fig. 3.1). This provided a representation of the displacement patterns and finger shapes (4) three breakthrough times (t_{br}) at R_1, R_2, and R_3 were recorded.

(4) the oil recovery percentage was calculated using equation 3.1 :

$$\%Rec = \frac{Qt_{br}}{\varepsilon h \pi r^2} \times 100 \tag{3.6}$$

(5) finally, to ensure reproducibility, the washing and drying processes of the cell were identical for each experiment. The washing process of the cell included the injection of one pore volume of hexane, followed by one pore volume of propanol-2, followed by two pore volumes of acetone.

The drying process of the cell was passing nitrogen gas slowly through the porous medium for 15-20 minutes, and evacuating the cell.

3.4.1 Preliminary Experiments

The main objectives of this study were to examine the effect of a spectrum of sodium hydroxide concentrations in the displacing phase on recovery percentage. and the effect of flowrate on recovery percentage.

To carry out these tasks, preliminary runs were done to investigate:

(1) the appropriate acid concentration in the oil phase (displaced phase)

(2) the suitable spectrum of sodium hydroxide (NaOH) concentration in the aqueous phase (displacing phase)

(3) if the minimum IFT value lies within the sodium hydroxide concentration range that was selected.

(4) pH, viscosity, and density of the sodium hydroxide solutions selected.

(5) whether or not the flowrate range discussed in this study includes all three regions (i.e capillary, intermediate and viscous region).

Table 3.3 gives the specification of the system used in this study:

Table 3.3: The specification of the system used in this work

Name	Specification	Remark
Sodium Hydroxide	Fisher Certified'ACS'Pellet	Used as Supplied
Light Paraffin Oil	BDH	Used as Supplied
Linoleic Acid	Fisher Reagent;Purified	Used as Supplied
Water	Double Distilled Water	Used as Supplied
Glass Beads	Rouville INC	Used as Supplied
Vacuum Pump	Can. Prod. Welch Co.	Used as Supplied

Chapter 4

Results and Discussion

4.1 Physical Properties of Aqueous and Oleic Solutions

4.1.1 Aqueous Phase

The physical properties required in this study (density, viscosity, and pH) were measured for all of the aqueous solutions. The density of pure water at room temperature ($25°C$) was 997.146 kg/m^3.

The pH values for the working aqueous solutions are plotted in Fig. 4.1

These values are very close to the theoretical values calculated in Eqs. 4.1 and 4.2.

$$pH = -log[H^+] \tag{4.1}$$

$$pOH = -log[OH^-] \tag{4.2}$$

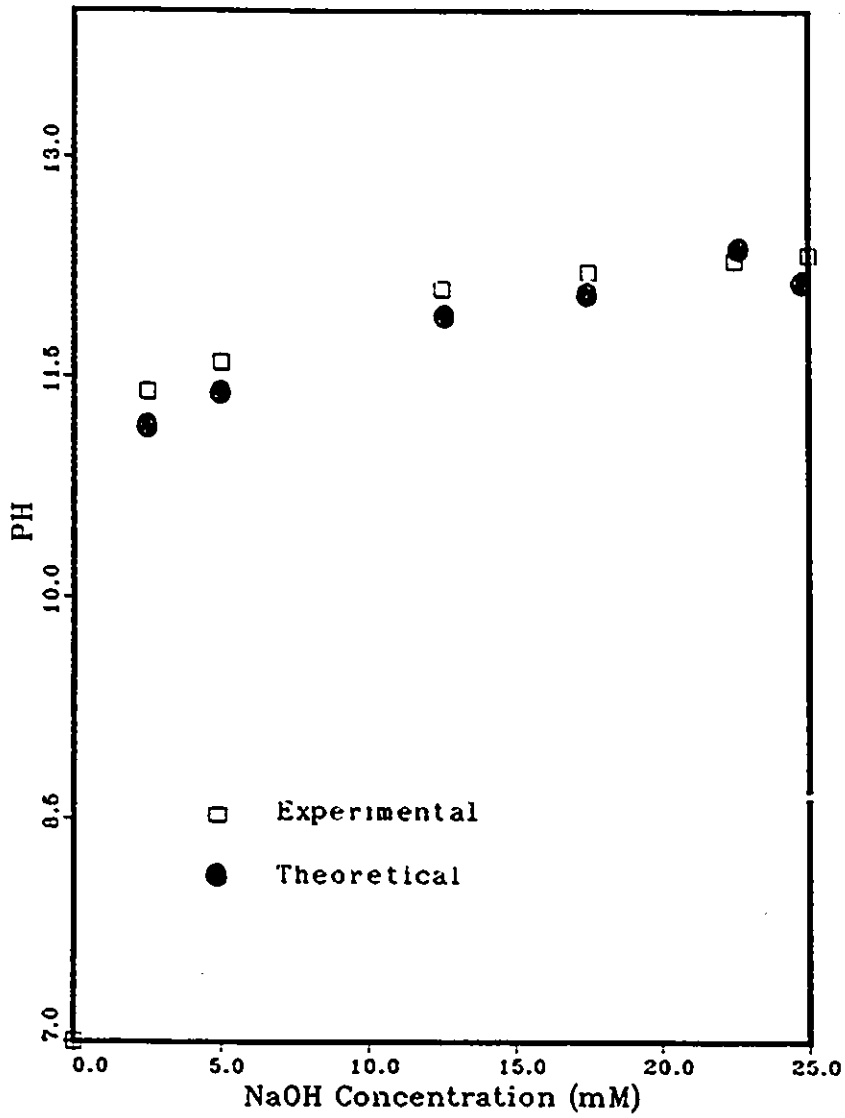

Figure 4.1: pH as a function of aqueous NaOH concentration

The viscosity data were obtained by using a Brookfield Synchroelectric Viscometer at different shear rates. As expected, the viscosities of the very dilute caustic solutions were almost independent of the NaOH concentration and were essentially the same as for pure water at the same temperature (i.e.,$1.0 \pm 0.05\ mPa.s$). Viscosity data for different sodium hydroxide solutions is given in table 4.1.

Table 4.1: Viscosity data for different NaOH solutions

NaOH concentration (mM)	Viscosity (mPa.S)
Pure water	0.891
2.5	0.892
12.5	0.895
25	0.896

4.1.2 Oleic Phase

The acidic oil utilized in this study was a 10.0 mM solution of linoleic acid in light paraffin oil which had a viscosity of 19.51 $mPa.s$ and a density of 857.0 kg/m^3.

4.2 Transient IFT Behavior of Oil/Caustic Interfaces

4.2.1 Effects of acid content of oleic phase

The effects of oil acidity on transient IFT's were experimentally investigated for systems with 10.0 mM linoleic acid dissolved in light paraffin oil, in contact with

varying concentrations of NaOH.

Upon contacting the acid with caustic solution, the IFT drops drastically on account of the initial formation of surfactant by reaction at the droplet surface. After the IFT reaches a minimum, it then increases steadily as the acid in the oil is gradually depleted by reaction. The IFT for 10.0 mM linoleic acid in contact with 12.5 mM NaOH solution reached its minimum value (0.26 mN/m) after 900 seconds contact time. At higher acid concentrations, lower IFT's were obtained but these required a longer contact time to become established. From this set of experiments, it can be concluded that the concentration of the acid in the oil is directly proportional to the interfacial activity. Generally speaking, the acid number of the oil (acid number is the milligram of potassium hydroxide required to neutralize the acid contained in one gram of oil sample) may be correlated directly with interfacial activity (Touhami et al. [36]).

4.2.2 Effects of varying alkaline concentration

The IFT data for 10.0 mM linoleic acid in light paraffin oil (which has an acid number of 0.56) in contact with 0.0 mM, 2.5 mM, 12.5 mM, and 25 mM aqueous NaOH solutions was measured with the Spinning Drop Tensiometer (SDT). Results are plotted in Figures 4.2, 4.3, and 4.4.

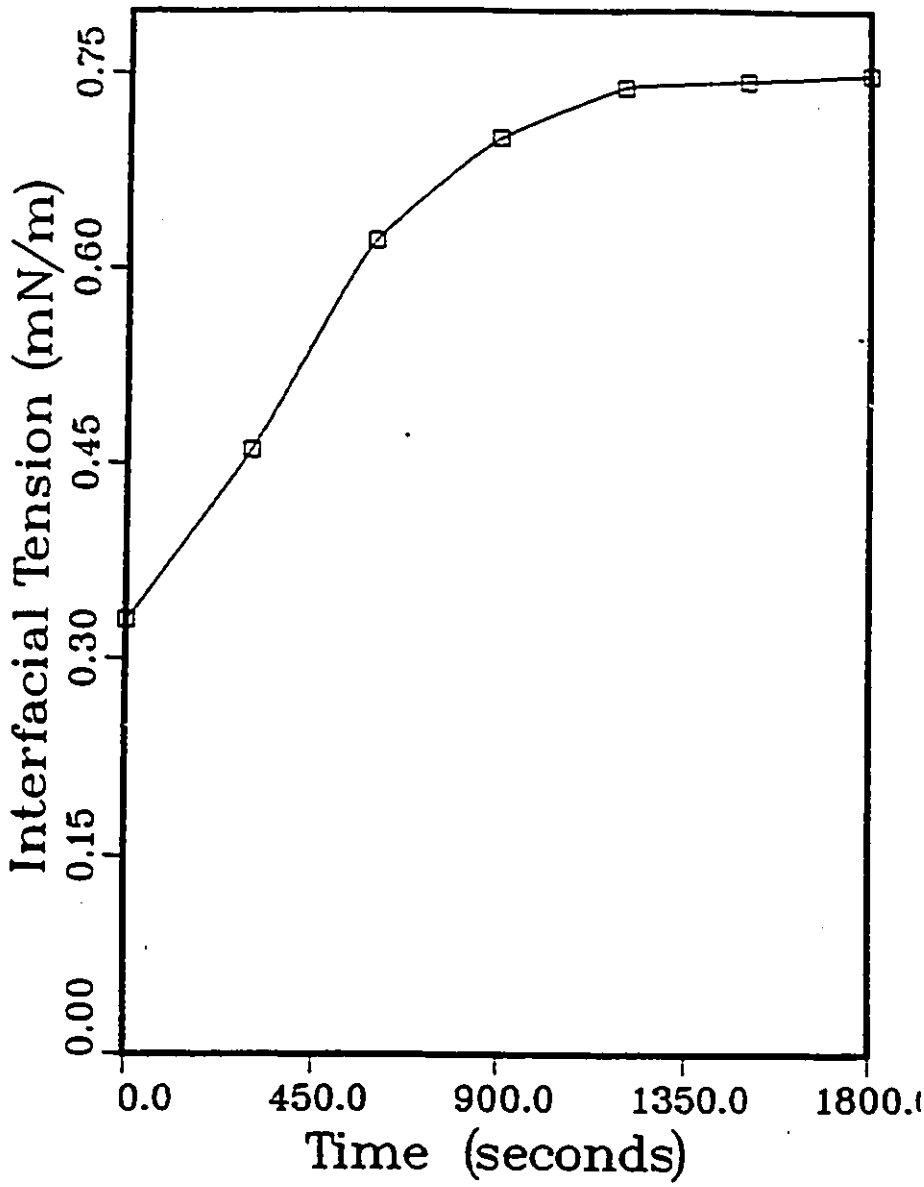

Figure 4.2: Dynamic IFT behavior of 10 mM acidic light paraffin oil against 2.5 mM NaOH solution

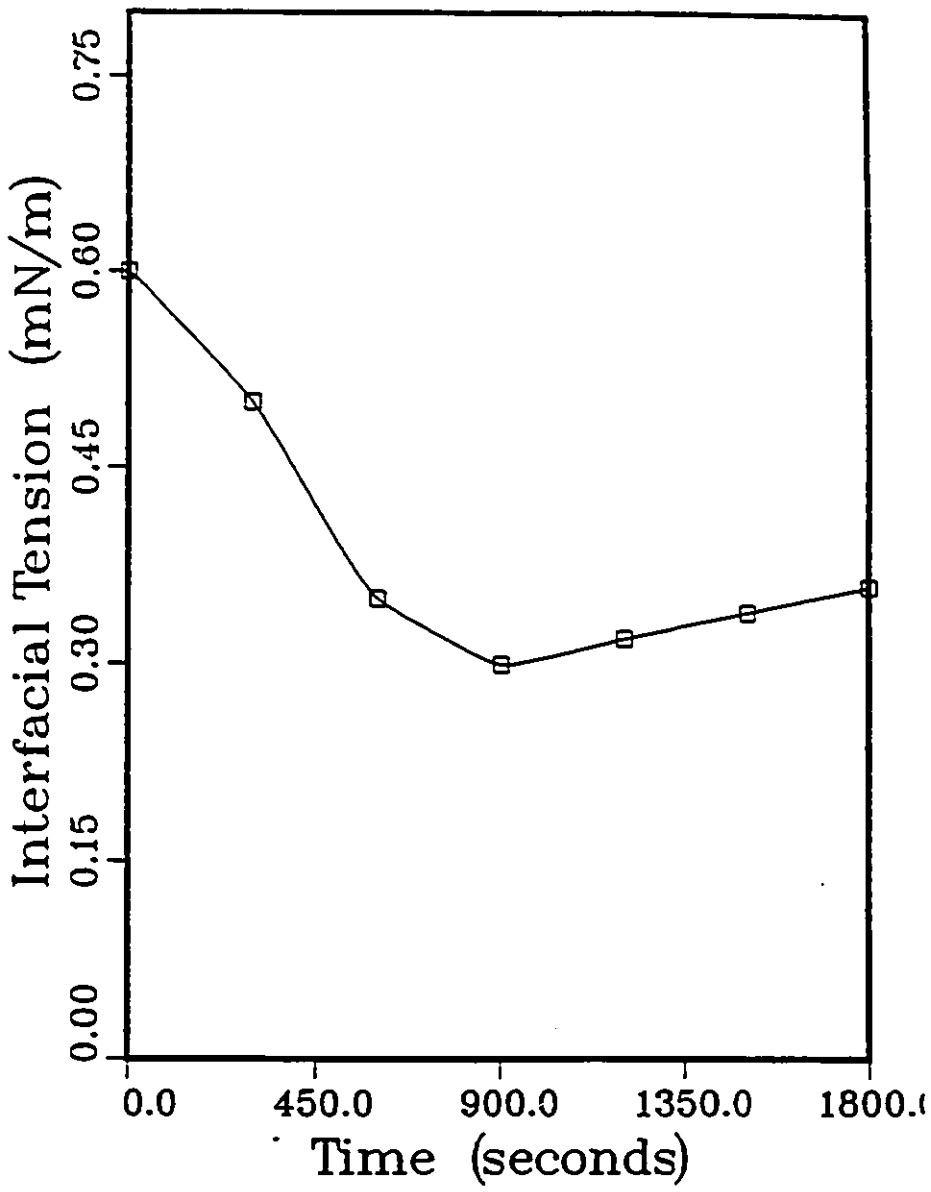

Figure 4.3: Dynamic IFT behavior of 10 mM acidic light paraffin oil against 12.5 mM NaOH solution

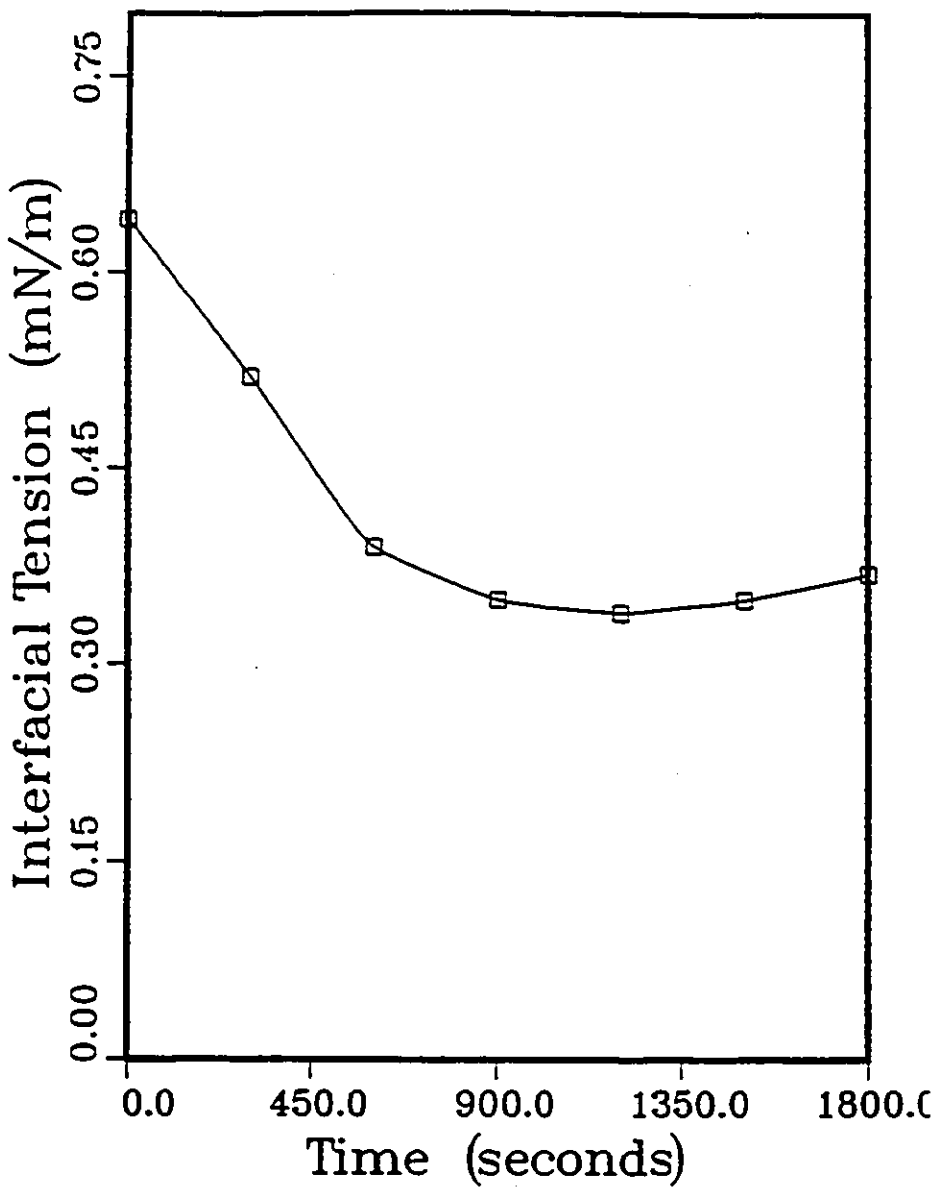

Figure 4.4: Dynamic IFT behavior of 10 mM acidic light paraffin oil against 25 mM NaOH solution

It was observed that the IFT value at equilibrium (i.e. after 1800 seconds contact time) for 2.5 mM, 12.5mM, and 25 mM NaOH are 0.78 mN/m, 0.2 mN/m, and 0.25 mN/m respectively. Figure 4.5 shows the minimum IFT at equilibrium for these three different concentrations.

It was observed that the IFT between pure water and acidic paraffin oil was 24 mN/m, while the IFT between pure water and pure light paraffin oil was 56 mN/m after 30 minutes contact time. This is because the acid in the oil phase behaves as a weak surfactant in neutral aqueous media, i.e. acidic oil has higher interfacial activity in contact with pure water than non-acidic oil with pure water.

The above measurements showed that low IFT values were obtained over the range between 2.5 mM and 25 mM caustic concentrations, results which are in good agreement with those of Chan et al. [16]. For this reason, the four NaOH concentrations of 0.0 mM, 2.5 mM, 12.5 mM, and 25 mM were used for all sets of experiments. Minimum IFT occurs at a certain NaOH concentration in the aqueous phase when in contact with a certain linoleic acid concentration in the oil phase. Sharma et al. [10] suggested that, once the pH value at the interface reaches the pK_a of the acid, the IFT drops to its minimum value, and the effective caustic concentration at which the interfacial pH approaches the pK_a value of the acid is between 2.5 mM and 25 mM NaOH concentration (for 10 mM acidic oil). The IFT measurements (Figs. 4.2, 4.3, and 4.4) indicate that the minimum IFT occurs at 12.5 mM NaOH concentration after 900 seconds contact time, because at this concentration the pH

at the interface reaches the pK_a value of the acid.

A further increase in NaOH concentration will cause a decrease in A^- ions at the interface by shifting the equilibrium to form undissociated soap (NaA), and consequently the IFT increases. Mingzhe et al. [37] suggested that the decrease in the concentration of A^- ions at the interface at high NaOH concentrations, is due to micelle formation and also to the suppression of electric double layers at higher ionic strengths. Fig. 4.5 shows IFT values at equilibrium (after 900 seconds contact time) for different NaOH concentrations.

4.3 Interpretation of Experimental Data

In order to interpret the results, one must have a good evaluation of

(1) IFT behavior in the region where interfacial reaction takes place, i.e. adsorption/ desorption of surface active species, and mass transfer of species to and from the interface due to diffusion and convection.

(2) Wettability conditions in the cell when the displacing phase come into contact with the displaced phase.

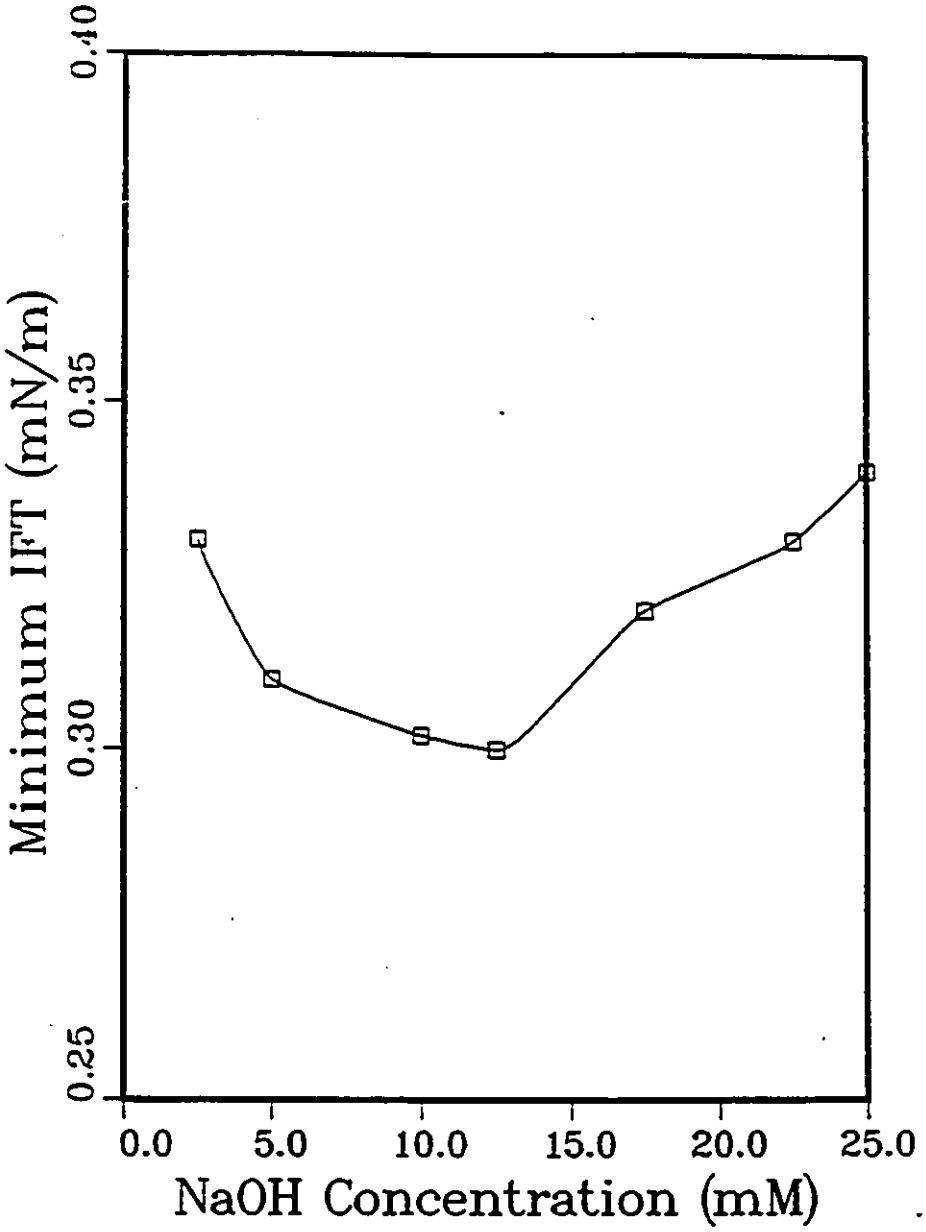

Figure 4.5: IFT of 10 mM acidic light paraffin oil against NaOH concentration at equilibrium (1800 seconds contact time)

On account of the preceding reasons, IFT behavior when measured with a Spinning Drop Tensiometer (SDT) is probably quite different from the behavior prevailing during actual water/oil displacement experiments. In the displacement the acidic oil comes into contact with caustic solution under very complicated conditions, and it is likely that equilibrium is not reached. This prevents the researcher from drawing quantative conclusions. Furthermore, since the system involves chemical reactions at the interface, the interpretation of the results is more complicated.

4.3.1 pH Change of Displacing Phase in the Cell at Different Radial Locations

As will be discussed later, experiments were conducted to confirm the reaction of species at the interface. These experiments assisted with the interpretation of the results. It is necessary to know the effects of chemical reaction on IFT behavior in the cell to properly interpret the data.

One can observe and fit the results of IFT measurements to match and support the oil recovery findings. Because of the above reasons, however, caution was exercised in relating experimental results solely to IFT measurements. To gain a better understanding of the experimental results, particularly in the capillary region (where the capillary forces are dominant at low flowrates and/or at high IFTs), one must prove existence of chemical reaction at the interface. Hence, experiments were

carried out to verify whether the acid in the oil reacted with the alkaline reactant at the interface, and if so, to what extent these reactions took place. To figure out IFT between two phases and pH value of NaOH solution, the most important step in this set of experiments is a reliable evaluation of the OH^- concentration at the oil/aqueous interface in the cell. To overcome this difficulty, a set of experiments was set up using a thymolphthalein indicator. The indicator changed color from blue to white near the 9.5 pH value. This color change was then related to the OH^- concentrations. With this procedure, even small changes in OH^- concentration were detectable at the interface, where acidic oil comes into contact with NaOH solution.

The first set of experiments was performed with 10 mM acid in light paraffin oil in contact with 2.5 mM NaOH solution containing 0.075% thymolphthalein as the displaced and displacing phases, respectively. The flowrate was constant at 3.3 ml/h (Fig. 4.6). All of the alkaline solution lost color from blue to white at the cell inlet, where the caustic solution initially came into contact with the acidic oil. This was because all of the OH^- concentration was exhausted at the early stage of the displacement process.

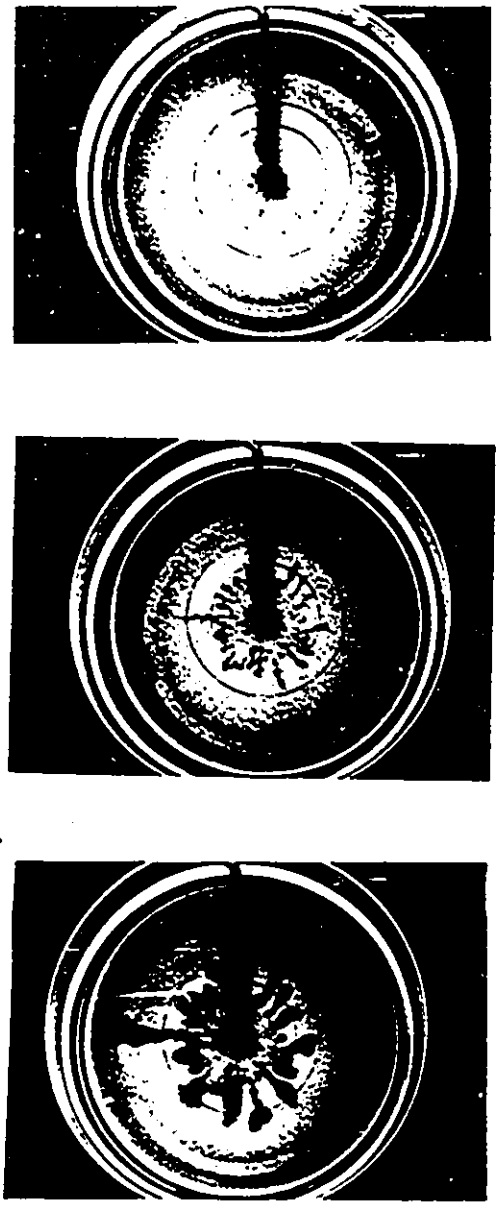

Figure 4.6: Fingering pattern for the case of 2.5 mM NaOH solution containing 0.075% thymolphthalein (appearing dark) displaces 10 mM linoleic acid in light paraffin oil at Q=3.3 ml/h and a capillary number of 2.4×10^{-6}

4.3.2 Analysis of Color Disappearance in the Cell

In section 4.3.1, experimental results showed that thymolphthalein in caustic solution loses its color when the pH value is less than 9.5. Fig. 4.1, where the pH value versus NaOH solution concentration is sketched, shows that 2.5 mM NaOH solution has a pH value of 11.2, which is blue in the presence of 0.075% thymolphthalein. If the NaOH solution is colorless(i.e. is not blue) the pH value of caustic solution is less than 9.5. In other words, the OH^- concentration decreases due to reaction with acid while all the NaOH is used up.

Two potential problems were identified while the above experiments were being carried out:

(1) the color change could not be detected in the cell because the blue alkaline solution lost all of its color at the initial contact (2) it was not known if the color disappearance was due to a chemical reaction or to color adsorption by the glass beads.

To elucidate the above problems, two special experiments were set up and run simultaneously. The first experiment was for a reacting system (test run I), while the second was for a non-reacting system (test run II) that had a higher caustic concentration. In this way , it was easier to observe the caustic color change in the cell. In the previous experiment, the NaOH concentration was very low, i.e. 2.5 mM

in the displacing phase, and all OH^- concentration would be used up from the cell inlet due to the chemical reaction. Hence, a higher concentration of NaOH solution was chosen for test run I and test run II. Test run I was performed with 5 mM of NaOH and 0.075% thymolphthalein in the displacing phase, and was brought into contact with 10 mM of acidic light paraffin oil. Test run II was performed under the same conditions as test run I, except that pure light paraffin oil was used as the displaced phase instead of acidic paraffin oil. Figs. 4.7 and 4.8 show the fingering patterns and the color changes for test run I (reacting system) and test run II (non-reacting system), respectively. Fig. 4.7 clearly demonstrates that caustic solution loses its color quite rapidly (in less than 500 seconds) when brought into contact with 10 mM acidic light paraffin oil. The color change is due to either chemical reaction and/or adsorption of the dye by glass beads inside the cell. However, test run II revealed that the color change was not due to adsorption. There was no color disappearance due to adsorption of dye by the glass beads inside the cell.

This series of experiments proves that the convective-diffusion and the chemical reaction decreased the OH^- concentration . This, in effect, caused the pH value to drop to a level where the blue caustic solution undergoes a color change from blue to white, i.e. less than 9.5 pH value (see Fig. 4.1).

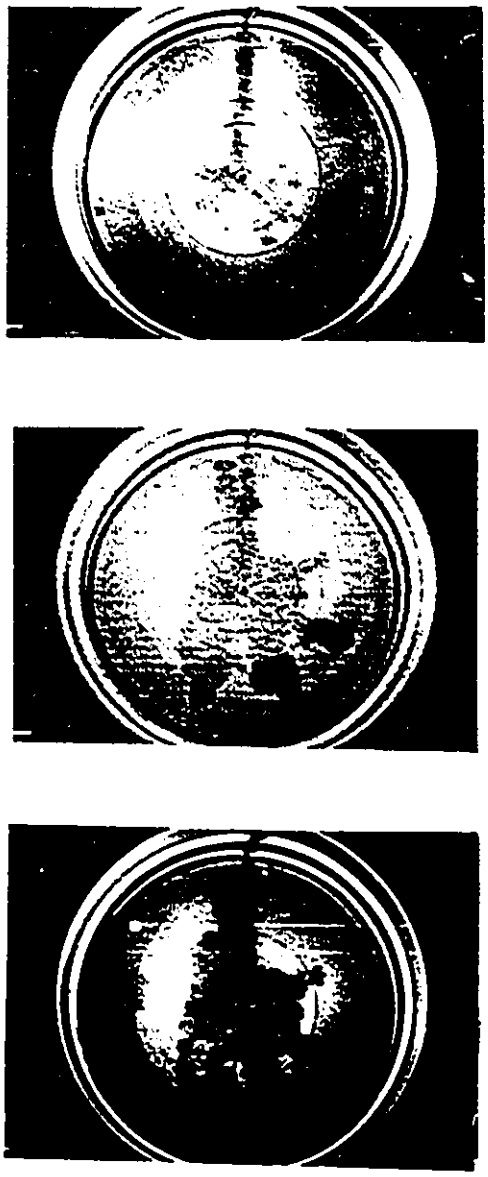

Figure 4.7: Fingering pattern for the case of 5 mM NaOH solution containing 0.075% thymolphthalein (appearing dark) displaces acidic oil at Q=3.3 ml/h and a capillary number of 4.8×10^{-6}

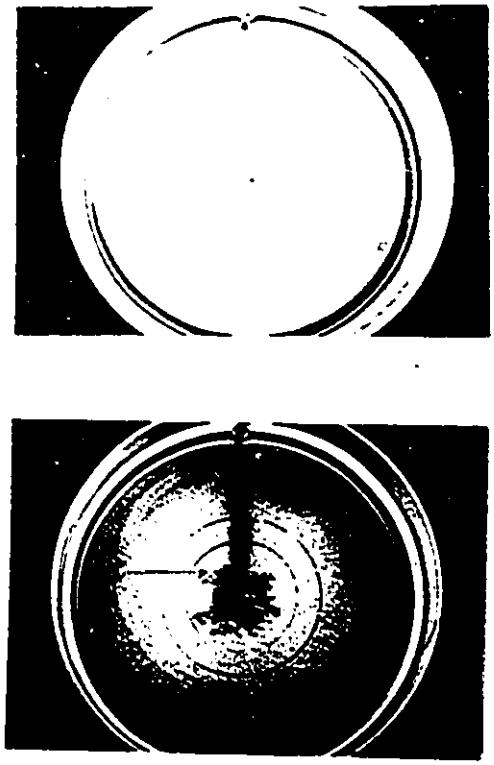

Figure 4.8: Fingering pattern for the case of 5 mM NaOH solution containing 0.075% thymolphthalein (appearing dark) displaces pure light paraffin oil at Q=3.3 ml/h and a capillary number of 2.8×10^{-6}

From the above two experiments, and using Fig. 4.1, it can be concluded that the NaOH concentration at the interface is less than 2.5 mM (pH value of a 2.5 mM solution is 11.2 which should be blue at 0.075% thymolphthalein concentration). Therefore, the IFT value of 2.5 mM NaOH solution in the cell is higher than that of 2.5 mM NaOH solution when measured with a Spinning Drop Tensiometer. This high IFT value is possibly a significant factor in decreasing the oil recovery percentage markedly.

The above experimental results indicate how the earlier contradictions faced in interpreting the recovery versus flowrate data will possibly be solved, where low recovery is observed at low IFT and high recovery is observed at high IFT (Fig. 4.9).

To support the result of test run I and test run II additional runs were done. In these new runs, either flowrate or concentration was increased. As the flowrate was increased to 5.5 ml/h under the same conditions as test run I (i.e. 5 mM NaOH concentration in the displacing phase coming into contact with 10 mM acidic oil), it was observed that the blue caustic solution lost less of its color than in test run I (Fig. 4.10).

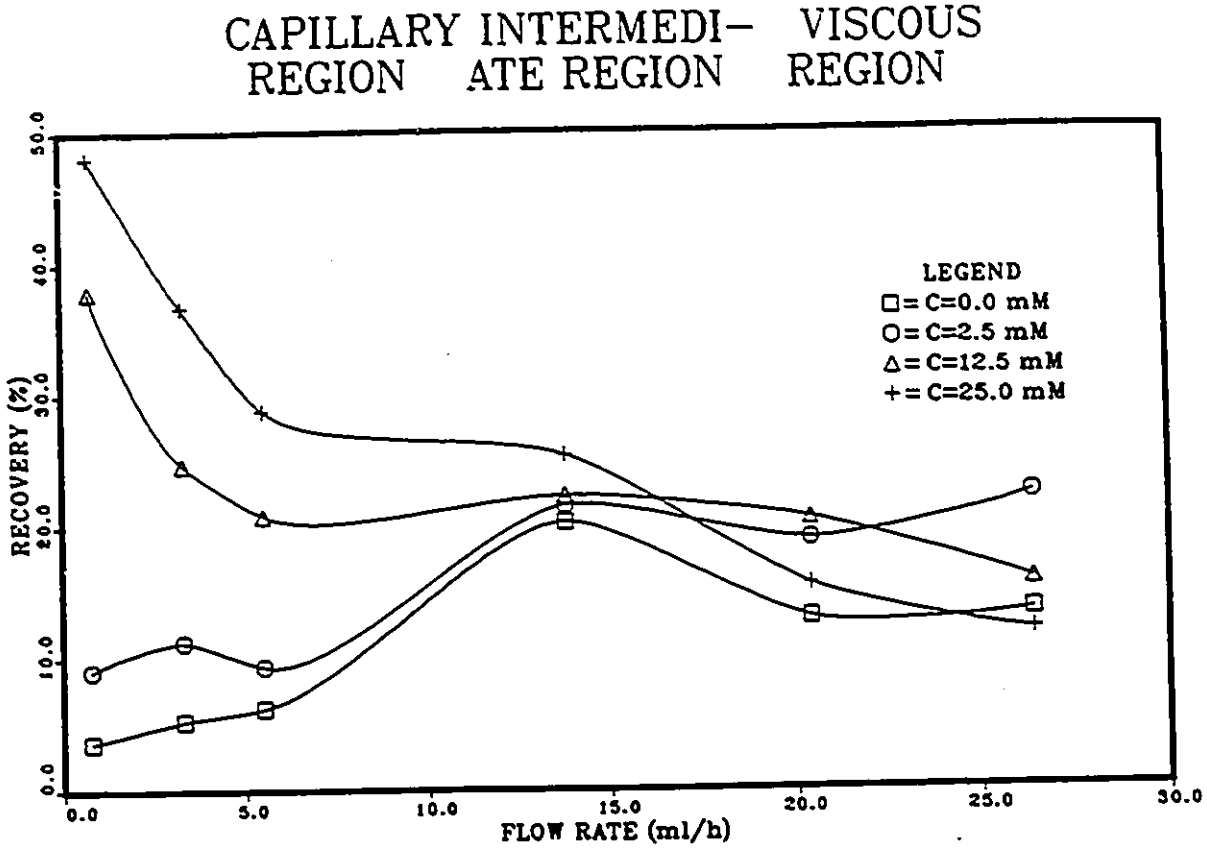

Figure 4.9: Effect of injection flowrate on the oil recovery percentage for different NaOH concentrations

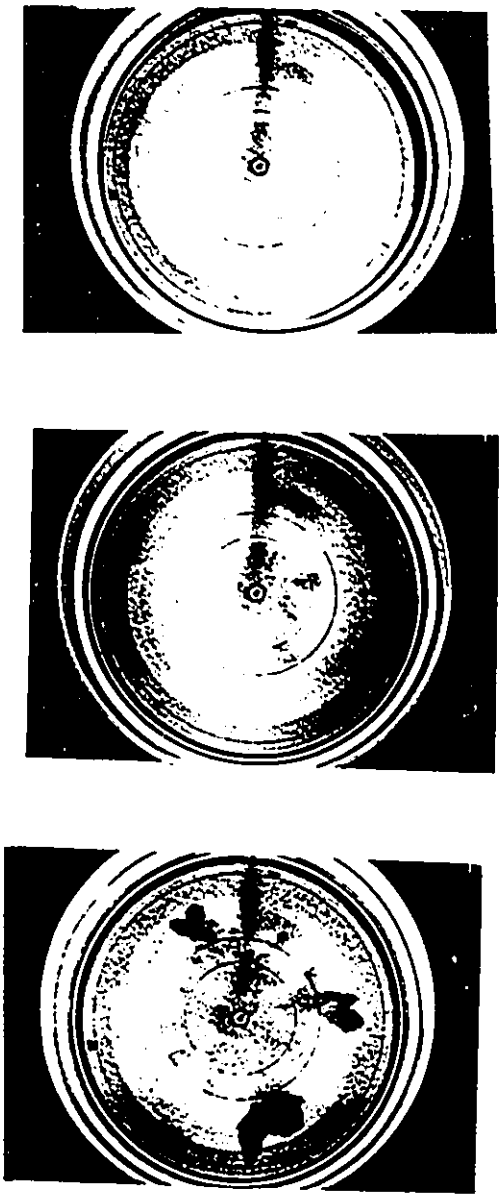

Figure 4.10: Fingering pattern for the case of 5 mM NaOH solution containing 0.1% thymolphthalein (appearing dark) displacing acidic oil at Q=5.5 ml/h and a capillary number of 8×10^{-6}

At a flowrate of 26.4 ml/h the blue caustic solution did not lose any of its color (Fig. 4.11). A possible explanation is that at higher flowrates, there is not enough time for convective-diffusion at the interface. This, in effect, keeps the caustic concentration high enough; this causes the pH value to remain at above 5mM at the cell exit point . Other sets of experiments were arranged with the same conditions as test run I, only with different alkaline concentrations. As the concentration of NaOH was increased to 12.5 mM with the same conditions as test run I, it was observed that, in comparison to test run I, the displacing phase lost less color at the tips of the fingers (Fig. 4.12). When a displacing phase of concentration 25 mM or higher is brought into contact with the acidic displaced phase, it is observed that the caustic solution color is fixed (Fig. 4.13). The reason is that at a higher concentration of caustic in the displacing phase, there are now enough OH^- ions available at the interface to react with all of the acid in the displaced phase. This, in turn, will keep the pH value high, and results in the observation of fixed caustic solution color.

Figure 4.11: Fingering pattern for the case of 5 mM NaOH solution containing 0.075% thymolphthalein (appearing dark) displaces acidic oil at Q=26.4 ml/h and a capillary number of 3.8×10^{-5}

Figure 4.12: Fingering pattern for the case of 12.5 mM NaOH solution containing 0.075% thymolphthalein (appearing dark) displaces 10 mM acidic oil at Q=3.3 ml/h and a capillary number of 1.04×10^{-5}

Figure 4.13: Fingering pattern for the case of 25 mM NaOH solution containing 0.075% thymolphthalein (appearing dark) displaces 10 mM acidic oil at Q=3.3 ml/h and a capillary number of 6.2×10^{-5}

4.4 Interpretation of Experimental Results Using Test Run I and Test Run II Conclusions

In run no. 4, NaOH with a concentration of 2.5 mM came into contact with 10 mM acidic light paraffin oil at a flowrate of 0.78 ml/h. It was observed that in the initial stages the displacing fluid (appearing dark) invades the displaced fluid through multi-directional tiny fingers, and that a single large, and more noticeable, finger grows in the direction of 6 o'clock (Fig. 4.14). Similar trends were observed in non-reacting linear systems (Perkin et al. [35]) and radial immiscible displacements (Nasr-El-Din et al. [32]), when a wetting fluid displaces non-wetting fluids in a porous medium.

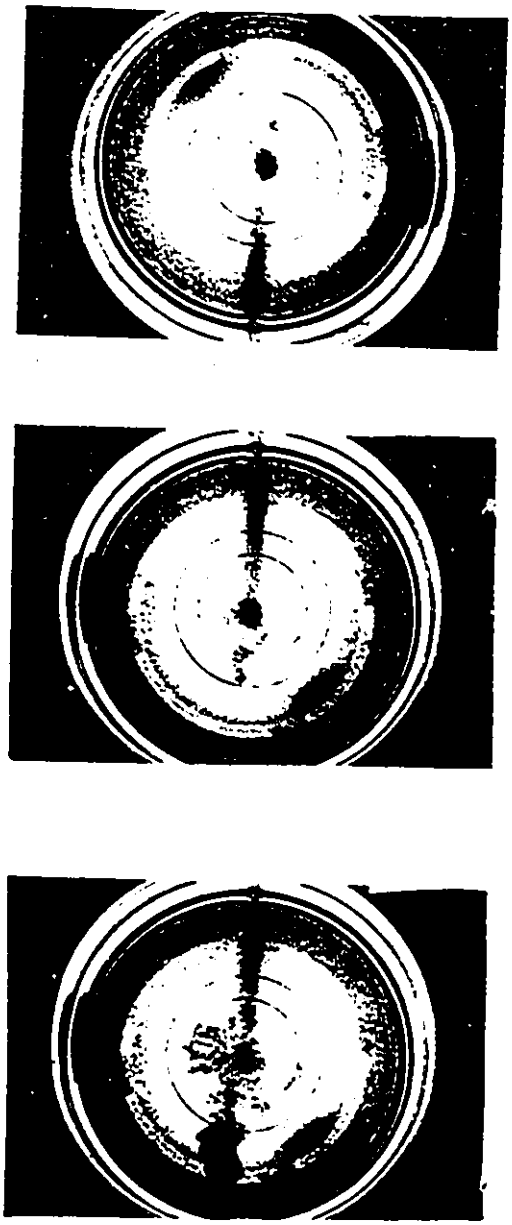

Figure 4.14: Fingering pattern for the case of 2.5 mM NaOH solution (appearing dark) displacing 10 mM acidic oil at Q=0.78 ml/h and a capillary number of 5.6×10^{-7}

4.4.1 Low Caustic Concentration in Contact with Acidic Oil in the Cell

When caustic solution of a low concentration is brought into contact with acidic oil (reacting system), the behavior observed is similar to that of non-reacting systems. where only pure water is used as the displacing phase (Fig. 4.9). D. A. Peru and P. B. Lorenz [38] stated that the alkali at low concentration requires uneconomically large injection volumes to survive in most reservoirs because of rapid consumption by acidic ions.

Results of test run I were discussed in chapter 4.3.2. Test run I at low concentration of NaOH demonstrated that most of the NaOH concentration is used up by reaction in the proximity of the interface with the acid in the oil phase. Hence, the NaOH concentration is lower than its initial value of 2.5 mM, especially at the cell exits between R_2 and R_3 (run no. 4, Fig. 4.14).

For this reason, in run no. 4 the IFT probably increased to a value much higher than its initial value (0.71 mN/m that was measured with SDT) therefore, the recovery percentage is kept at a low percentage similar to run no. 13 (i.e. same condition as run no. 4, but instead of using 2.5 mM NaOH solution, pure water was used as the displacing phase) which is a non-reacting system, see Fig. 4.15.

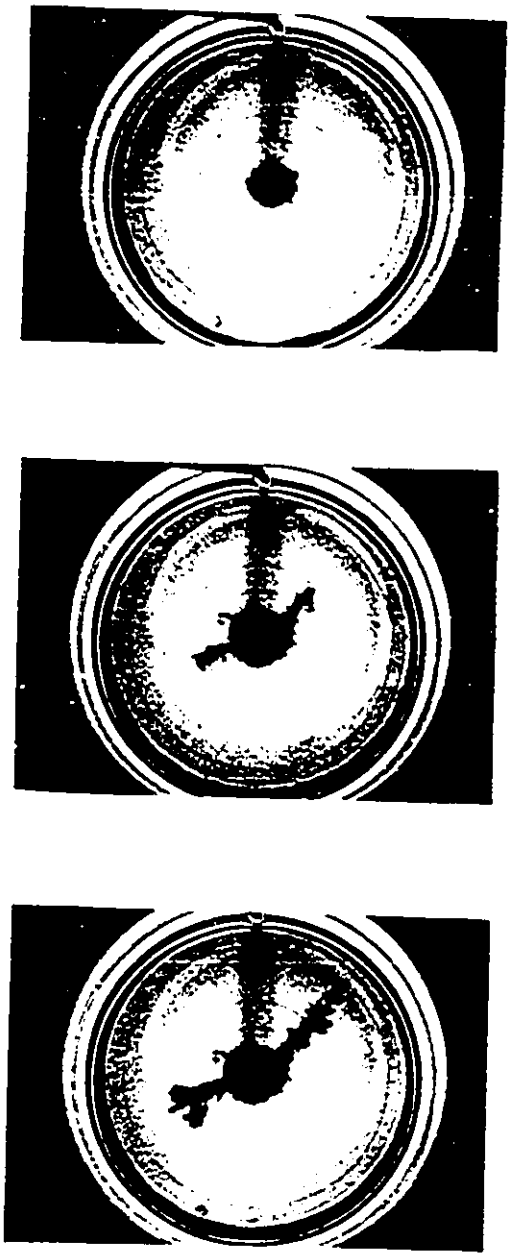

Figure 4.15: Fingering pattern for the case of pure water solution (non-reacting system) displacing 10 mM acidic oil at Q=0.78 ml/h and a capillary number of 5.7×10^{-7}

4.4.2 High Caustic Concentration in Contact with Acidic Oil in the Cell

In this set of experiments, higher concentration of NaOH solution were used . In run no. 7 (Fig. 4.16) and run no.2 (Fig. 4.17), the NaOH concentrations were 12.5 mM for run no. 7 and 25 mM in run no.2, while the flowrate was a constant 0.78 ml/h. Fig. 4.9 shows that much higher recovery rate was obtained when using 25 mM of caustic solution (run no. 7), rather than 12.5 mM caustic solution (run no. 2). However, Fig. 4.5 shows that when the IFT was measured with a Spinning Drop Tensiometer, the 12.5 mM NaOH solution in contact with 10 mM acidic light paraffin oil had the lowest IFT value after 900 seconds contact time. Therefore a higher recovery percentage is expected for 12.5 mM NaOH solution rather than for 25 mM NaOH solution. This contradiction was previously mentioned in the discussion of test run I and test run II. Although 12.5 mM caustic solution was injected into the cell as the displacing phase, the NaOH was depleted by reaction, i.e. the NaOH concentration decreased to less than 12.5 mM, the reason behind that could be either convective-diffusion of NaOH into the oleic phase and/or chemical reaction at the interface. Fig. 4.5 shows that as the NaOH concentration in the aqueous phase decreases, the IFT value shifted to a higher value inside the cell because of the NaOH depletion at the cell interface, that is why the 12.5 mM NaOH solution in contact with acidic oil in the cell did not have minimum IFT.

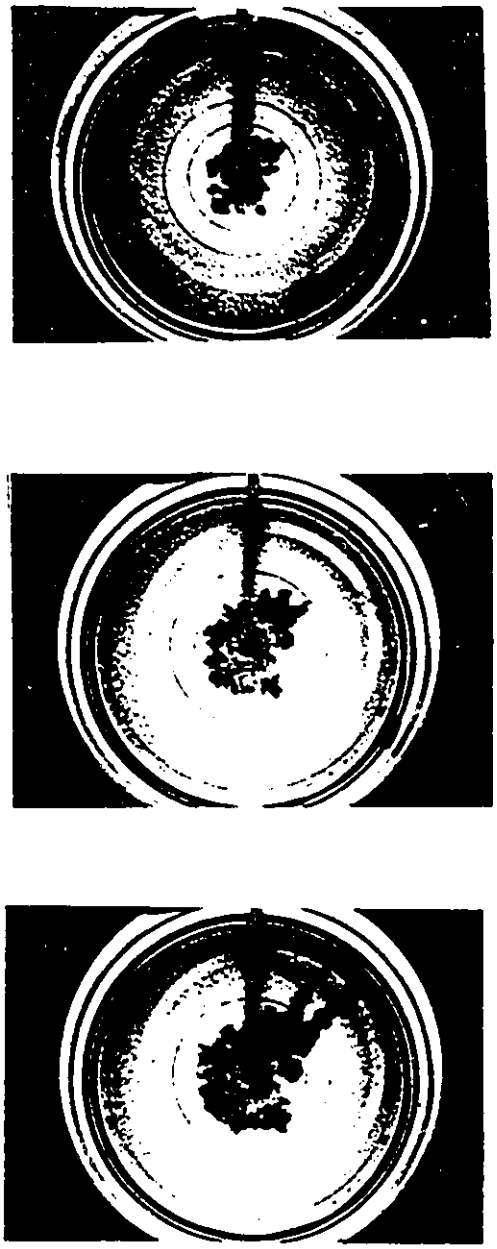

Figure 4.16: Fingering pattern for the case of 12.5 mM NaOH solution (appearing dark) displacing 10 mM acidic oil at Q=0.78 ml/h and a capillary number of 1.13×10^{-6}

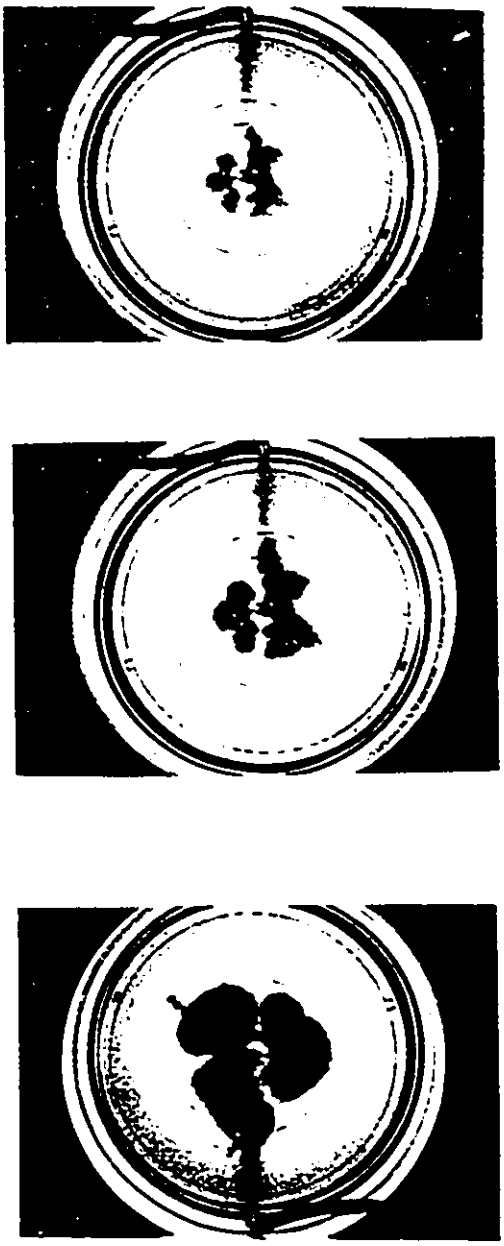

Figure 4.17: Fingering pattern for the case of 25 mM NaOH solution (appearing dark) displacing 10 mM acidic oil at Q=0.78 ml/h and a capillary number of 1.5×10^{-5}

This contradiction can also be interpreted in terms of wettability condition. As discussed in chapter 2.3.5, alkaline solution may cause wettability alteration. For this system (10 mM acidic oil in contact with different NaOH concentrations in porous medium), the highest recovery is obtained at 0.78 ml/h flowrate. This implies that the optimum wettability condition possibly occurs at these conditions. For run no. 2, where the NaOH concentration was 25 mM, the actual NaOH concentration was less than 25 mM at the interface (due to convective diffusion and/or chemical reaction). Fig. 4.5 shows that as the NaOH concentration decreased toward 12.5 mM at the interface, the IFT was decreasing towards its lowest value. These reasons cause a higher recovery percentage value to be observed for 25 mM NaOH concentration, which has a higher IFT than the 12.5 mM concentration.

Table 4.2 shows the experimental results of run no. 7 and run no. 2.

Table 4.2: Experimental result of run no. 7 and run no. 2

Run no.	NaOH concentration	Flowrate	Breakthrough time	Recovery
	mM	ml/h	second	%
7	12.5	0.78	31500	38
2	25	0.78	40000	48

To further support these results, two higher flowrates were used (run no. 6 and run no. 1). The NaOH concentrations were 12.5 mM (run no. 6) and 25 mM (run no. 1) respectively, but the flowrate was 5.5 ml/h for both runs.

Table 4.3 shows the experimental results of run no. 6 and run no. 1.

Table 4.3: Experimental result of run no. 1 and run no. 6

Run no.	NaOH concentration	Flowrate	Breakthrough time	Recovery
	mM	ml/h	second	%
1	12.5	5.5	2450	29
6	25	5.5	3390	20

Comparing run no. 6 (Fig. 4.18) with run no. 1 (Fig. 4.19) and using Fig. 4.9. it is apparent that a higher recovery percentage is obtained for higher IFT value (i.e. 25 mM NaOH concentration). However, Fig. 4.9 shows that the recovery percentage difference between run no. 2 and run no. 7 is 15%. This value is much higher than the 7.8% recovery percentage difference observed between run no. 6 and run no. 1. The reason for this lower recovery percentage is that run no. 6 and run no. 1 were done at a higher flowrate (5.5 ml/h), where the contact time was not as long as in run no.7 and run no. 2 (since the flowrate was slower). Consequently, there was not enough time for chemical reaction to take place and the OH^- concentration did not decrease substantially at the interface. Therefore, in both runs (i.e. 12.5 mM and 25 mM NaOH concentrations) the OH^- concentration at the interface did not decrease markedly. To increase the IFT of 12.5 mM NaOH solution considerably or to decrease the IFT of 25 mM NaOH solution toward the least IFT value, it is possible that the chemical reaction at the interface inside the cell might change the IFT to the extent that the IFT of 25 mM NaOH solution is less than that of

12.5 mM NaOH solution when contacting with 10 mM acidic oil. However, the IFT difference between run no. 6 and run no. 1 is less than that of run no. 7 and run no. 2. Alternatively, one could say that the wettability condition is still more favorable for 25 mM NaOH concentration than for 12.5 mM NaOH concentration, due to the pH of 25 mM NaOH solution being higher than that of the 12.5 mM NaOH concentration.

Fig. 4.9 shows that as the flowrate increased to 13.8 ml/h, the recovery percentage difference for all the concentrations (2.5 mM ,12.5 mM, and 25 mM NaOH) decreased towards 5%. It was observed that for the entire set of experiments for flowrates at and above 13.8 ml/h the breakthrough time (t_{br}) is about 500 seconds. In this time period, the IFT value for all the above concentrations are between 0.38 mN/m and 0.47 mN/m. Figs. 4.2, 4.3, and 4.4 shows that due to high flowrates of the displacing phase , and consequently very short contact time, there was always enough fresh NaOH present at the interface to prevent the IFT changing substantially. This is in contrast to the low flowrate (capillary region) observations.

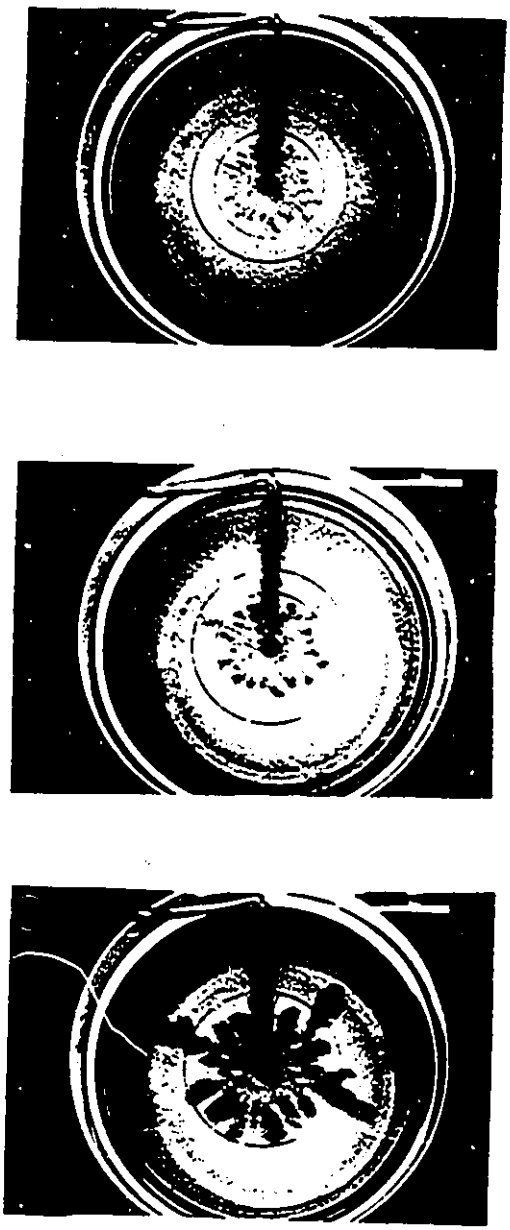

Figure 4.18: Fingering pattern for the case of 12.5 mM NaOH solution (appearing dark) displacing 10 mM acidic oil at Q=5.5 ml/h and a capillary number of 1.7×10^{-5}

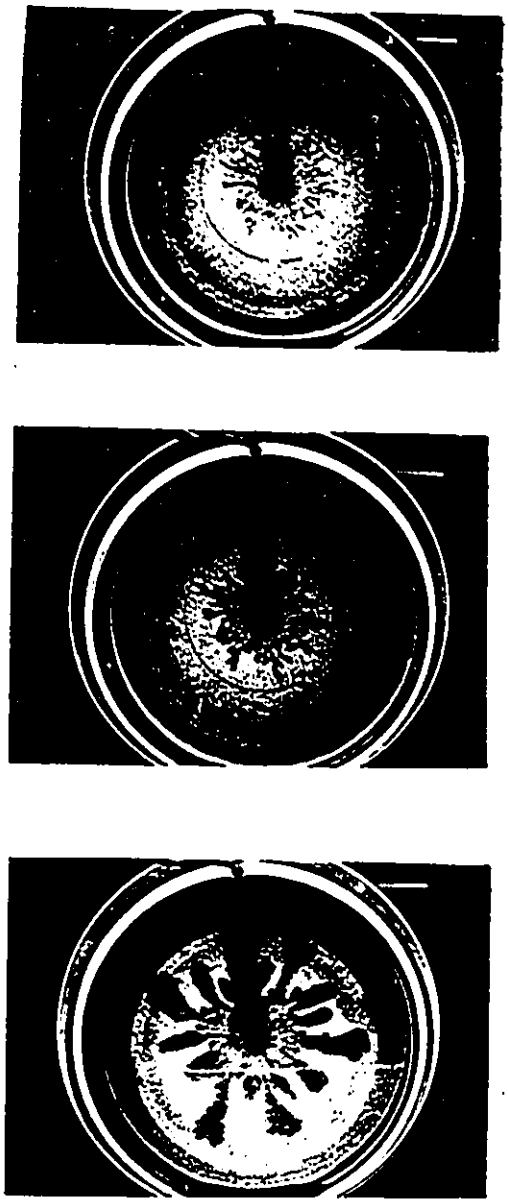

Figure 4.19: Fingering pattern for the case of 25 mM NaOH solution (appearing dark) displacing 10 mM acidic oil at Q=5.5 ml/h and a capillary number of 1.04×10^{-4}

4.5 Effect of Capillary Number (N_{ca}) on Displacement Pattern and Finger Shape

4.5.1 Effect of Flowrate on Recovery Percentage

Fig. 4.9 shows that for the NaOH concentration of 12.5 mM and 25 mM, the flowrate was inversely proportional to the recovery percentage. This means that in the capillary region, where the flowrates are low, the capillary forces are dominant because of spontaneous imbibition. In this region, a higher recovery percentage was observed than that obtained in the viscous region where the flowrates are high and viscous forces are dominant.

The above observation can be explained by examining the water wet porous medium (the case of our interest) in the capillary region. In this region the capillary number ($N_{ca} = \mu V/\varepsilon\gamma$) is low (i.e. either low flowrate and/or high IFT). The displacing phase passes through pores of small diameter where the capillary pressure is high (spontaneous imbibition).

In contrast to the capillary region, in the viscous region (where the flowrates are high and the viscous forces are dominant), the displacing phase has a tendency to pass through large pores where the capillary pressure is small.

As r (radius of fingers) increases, the linear velocity decreases together with the

viscous forces. Since the capillary number is proportional to th velocity, and lower the capillary number is, more dominant capillary forces become, therefore capillary forces become larger at the cell exit than those at the cell inlet. This means the capillary number is not constant at the different radius of the cell.

Fig. 4.9 shows that when flowrate increases in the capillary region, recovery percentage decreases. Increasing the flowrate from 0.78 ml/h to 3.3 ml/h (at 25 mM and 12.5 mM NaOH concentration) had an inverse effect on recovery percentage, which decreased from 50% to 37%. This was because capillary forces are less dominant at higher flowrates.

As a result of increasing the flowrate (Q) up 13.8 ml/h from 0.78 ml/h (with the same concentration of 25 mM NaOH in the viscous region) where the viscous forces are dominant, the recovery percentage decreased to 24.5%.

In the viscous region, the recovery percentage was not sensitive to the flowrate. In contrast, in the capillary region the recovery percentage is highly sensitive to the different flowrates. It was observed that in the viscous region, the difference of recovery percentage divided by the difference of flowrate was almost zero ($dRec/dQ = 0$). This result is consistent with Nasr-El-Din et al.'s [32] findings.

4.5.2 Effect of Flowrate on Displacement Pattern

When a caustic solution of low concentration (such as 2.5 mM) was brought into contact with acidic oil at a very low flowrate (0.78 ml/h, i.e. in the capillary region where the capillary number is low, 5.7×10^{-7}), one finger was observed to grow dominantly, (run no. 4, Fig. 4.14). This is due to imbibition. The behavior is called the shielding effect, and was also observed by Homsy [39] and Nasr-El-Din et al. [32].

Run no. 9 (see Fig. 4.20) was carried out with the same concentration as run no. 4 but at a higher flowrate (i.e. 26.4 ml/h). In run no. 9, the capillary number was 1.9×10^{-5} which is almost 30 times higher than that of run no.8. This explains the increase in the number of fingers, and the thinner tips of the fingers than those of run no. 4 (see Fig. 4.20). This behavior is called the splitting effect: this trend was observed in linear displacements by Perkins et al. [35] and in radial displacements by Nasr-El-Din et al. [32].

Experimental results showed that the displacement patterns and shapes of fingers were greatly dependent on the capillary number (N_{ca}). When comparing run no. 4 (Fig. 4.14, which is in the capillary region) with run no. 9 (Fig. 4.20, which is in the viscous region), the imbibition phenomenon was only observed in the capillary region.

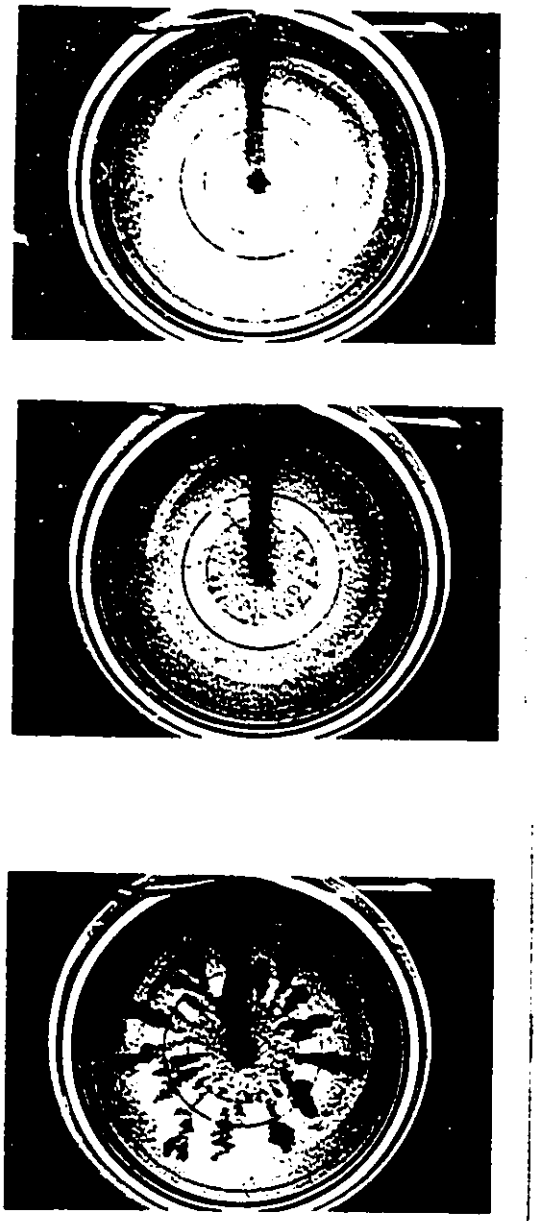

Figure 4.20: Fingering pattern for the case of 2.5 mM NaOH solution (appearing dark) displacing 10 mM acidic oil at Q=26.4 ml/h and a capillary number of 9.9×10^{-7}

4.5.3 Effect of NaOH Concentration on Displacement Pattern and Finger Shape

In the previous section, the results implied that the displacement patterns were highly dependent on the capillary number. When the concentration of NaOH in the displacing phase changes, it seems as though the capillary number changes. This in turn means that a change in concentration will lead to different displacement patterns. With an NaOH concentration of 2.5 mM as the displacing phase, the IFT at the early stage of displacement process increased to a value of about 26 mN/m (IFT of pure water in contact with 10 mM acidic oil). This was a consequence of the rapid consumption of NaOH that took place at the interface (Peru et al. [39]). Therefore, at a high IFT value, the capillary number decreased to a lower value than 1.9×10^{-5}) (i.e. 5.6×10^{-7} at the flowrate of 0.78 ml/h, run no. 4, Fig. 4.14). Fig. 4.14 shows that one finger grows dominantly. However, at higher concentrations of NaOH (i.e. 25 mM) with the same flowrate (0.78 ml/h, run no. 2, Fig. 4.17). since the IFT value inside the cell was approaching the minimum IFT value of 0.3 mN/m, the capillary number increased to 1.5×10^{-5}.

Fig. 4.17 shows that the number of fingers was higher than in run no.8 (Fig. 4.14) and the fingers are thinner than those in Fig. 4.14.

4.5.4 Effect of Viscosity on Displacement Patterns

Section 1.3 and 2.5 explains why is it that a less viscous fluid has a tendency to finger through a more viscous fluid. When the less viscous fluid displaces a more viscous fluid, the case for displacement is unfavorable (i.e.when the viscosity ratio $\mu_o/\mu_w \geq 1$).

Conversely, when a less viscous fluid is being displaced by a fluid with high viscosity , the displacement pattern occurs in a stable circular fashion, i.e. no finger is observed (Fig. 4.21). This case is a favorable one (i.e. when viscosity ratio is $\mu_o/\mu_w \leq 1$).

4.5.5 Effect of Wettability Alteration on Recovery Percentage

Fig. 4.22 shows that as the pH value increases, the recovery percentage increases correspondingly for all three different flowrates in the capillary region. For example, the highest recovery percentage results at the highest pH value (12.38) and the lowest flowrate (0.78 ml/h).

The reason is that at a low pH value of aqueous solution, sodium hydroxide (NaOH) is consumed rapidly at the interface of the displacing phase and displaced

phase. Therefore, in this case, the IFT value is high enough ($> 20\ mN/m$) not to enhance recovery percentage: in addition, the wettability condition of the system at low pH values does not alter appreciably in porous medium (in contrast to high pH values). In other words, optimum wettability conditions generally occur at high pH values.

Fig. 4.22 also shows that the lower the flowrate, the higher the recovery percentage. Section 4.5.1 discusses that the capillary forces are more dominant at low flowrates than at high flowrates; therefore, the imbibition at low flowrate leads to high recovery percentages.

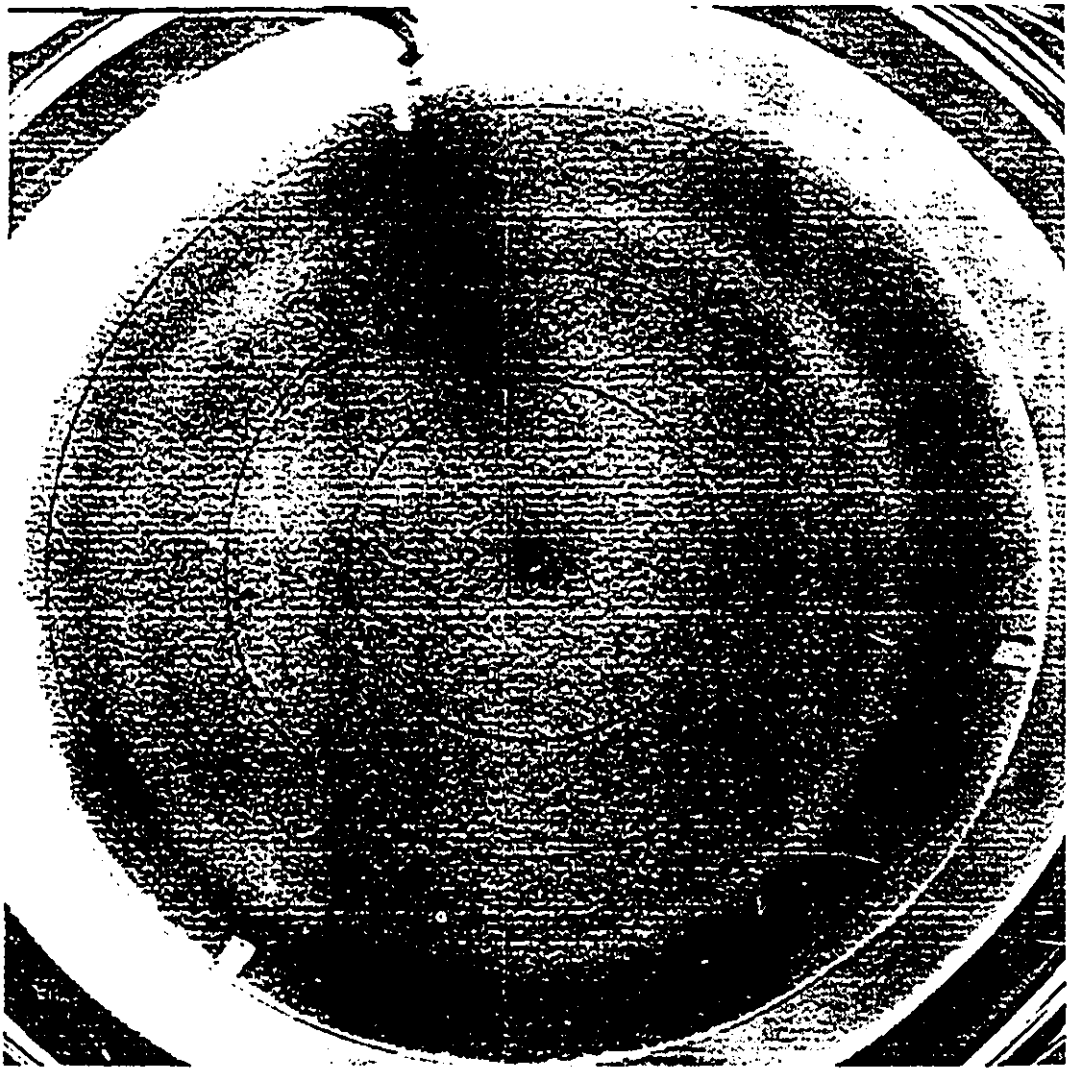

Figure 4.21: Fingering pattern for the displacement of 10 mM acidic oil (appearing dark) displacing 2.5 mM NaOH at Q=26.4 ml/h

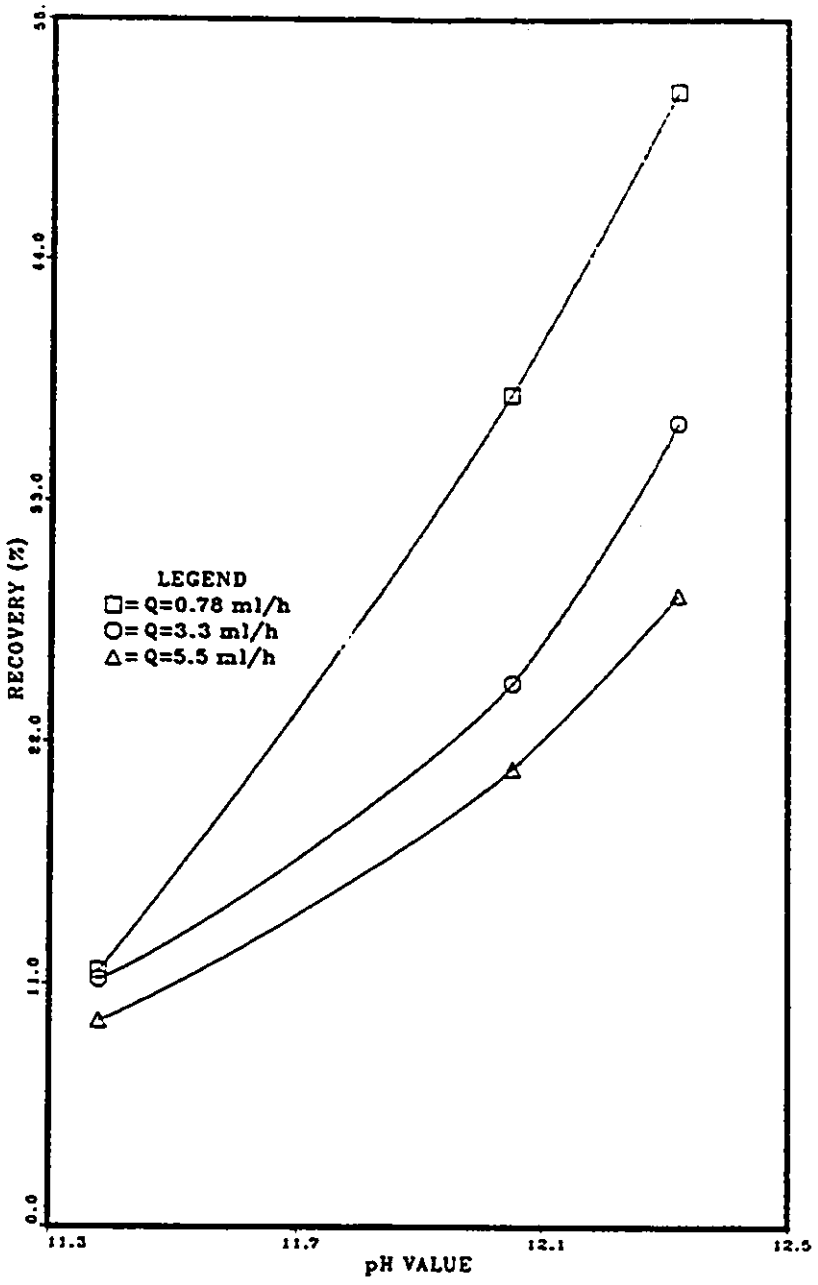

Figure 4.22: Recovery percentage as a function of pH for different flowrates

Chapter 5

Conclusions

It is confirmed that the addition of the sodium hydroxide to the aqueous phase reduces the interfacial tension between the aqueous phase and acidified oleic phase phase to ultra-low value. The IFT reduction which is a consequence of chemical reaction at the interface improves the recovery percentage.

The recovery percentage of the reacting system is found to be a function of the alkaline concentrations, flowrates, and wettability conditions.

It is also concluded that at very low NaOH concentrations, the recovery percentage versus flowrate curves behave like a non-reacting system. The different displacement patterns between reacting systems and non-reacting systems are observed. These different patterns for the reacting system are a consequence of IFT reduction, high pH value of aqueous solutions, and wettability alterations. The experiments show that the displacement patterns are a strong function of the capillary

number.

Minimum IFT measured with a spinning drop tensiometer for a certain concentration of NaOH in the aqueous phase and acid in the oil phase does not imply minimum IFT behavior in the cell (where the caustic solutions came into contact with the acidic oil).

Bibliography

[1] Taber, J.J.: *" Research on Enhanced Oil Recovery,"* Pergamon Press, 52, 1323-1347, Great Britain (1980).

[2] Seifert, W.K.: *"Progress in the Chemistry of Natural Products,"* W.Hertz, H.Griesbach and G.W.Kirby, Eds, Springer-Verlag, New York, Vol. 1 (1975).

[3] Parker, R.J. and E.S.N. Chung: *" Acid Number of Saskatchewan Heavy Oil,"* JCPT, 25, 72-75 (1986).

[4] MacKenzie, A.S., G.A. Wolff and J.R. Maxwell: *Advances in Organic Geochemistry,"* Bjory, M., Editor, Willey, London (1983).

[5] Ni, L.W., V. Hornof and G.H. Neale: *" Radial Fingering in a Porous Medium,"* Revue de l'Institut Francais du Petrole, 41, 217-228 (1986).

[6] Eldrich, R., H.H. Hasiba and P. Raimondi: *"Alkaline Waterflooding for Wettability Alteration-Evaluating a Potential Field Application,"* J.Pet.Tech., 26, 1335-1343 (1974).

[7] McCaffery, F.G.: *"Interfacial Tension and Aging Behaviors of Some Crude Oils Against Caustic Solutions,"* J.Pet.Tech., 28, 71-74 (1976).

[8] Kelly, J.G.: *"Tertiary Displacement of Oleic Acid Oils with Alkaline Agents,"* M.S. Thesis, U. of California-Berkley (1979).

[9] Chiwetelu, C.I.: *"Dynamic Interfacial Tension of Finite Reactive Systems Related to Enhanced Oil Recovery,"* Ph.D. Thesis, U. of Ottawa, Chemical Engineering Dept., Canada (1988).

[10] Sharma, M. M. , L.K. Jang and T.F. Yen: *" Transient Interfacial Tension Behavior of Crude Oil Caustic Interfaces "*, SPERE, 4, 377-389 (1989).

[11] DeZabala, E.F., J.M. Vislocky, E. Rubin and C.J. Radke: *" A Chemical Theory of Linear Alkaline Flooding ,"* Trans. SPE of AIME , 245-258 (1982).

[12] England, D.C. and J.C. Berg: *" Transfer of Surface-Active Agents Across a Liquid-Liquid Interface ,"* AIChEJ., 17, 313-322 (1971).

[13] Rubin, E. and C.J. Radke: *"Dynamic Interfacial Tension Minima in Finite System,"* Chem. Eng. Sci., 35, 1129-1138 (1980).

[14] Ramakrishnan, T.S. and D.T. Wasan: *"A Model for Interfacial Activity of Acidic Crude Oil/Caustic System for Alkaline Flooding,"* SPEJ., 23, 602-612 (1983).

[15] Guastala, L. P. and J. Guastalla: *"Influence de la Temperature Sur la Pression des Couches d'Asorption Gazeuses D'Alcools Aliphaliques,"* J. Chim. Phys., 56, 867-872 (1959).

[16] Chan, M. and T.F. Yen: *"A Chemical Equilibrium Model for Interfacial Activity of Crude Oil in Aqueous Alkaline Solution: The Effect of pH. Alkali and Salt,"* Can. J. Chem. Eng., 60., 305-308 (1982).

[17] Trujillo, E.M.: *"The Static and Dynamic Interfacial Tension between Crude Oil Caustic Solutions,"* SPEJ, 23, 125-134 (1983).

[18] Sinclair, D. and V.K. La Mer: *" Light Scattering as a Measure of Particle Size in Aerosole,"* Chem. Rev., 44, 245-67 (1949).

[19] Cockbain, E.G. and J.H. Schulman: *" Molecular Interaction at Oil/Water Interfaces,"* Trans. Faraday Soc., 36, 165-168 (1940).

[20] Bartell F.E., W. Charles and J.R. Walton: *"Alteration of the Surface Properties of Stibnite as Revealed by Adhesion Tension Studies,"* Chemical Laboratory, University of Michigan, Ann. Arbor, Michigan, 503-511 (1933).

[21] Morrow, N.R.: *"Wettability and Its Effect on Oil Recovery,"* J.Pet.Tech., 42, 1476-1469 (1990).

[22] Cook, C.E. Jr., R.E. William and P.A. Kolodzie: *" Oil Recovery by Alkaline Flooding,"* J.Pet.Tech., 1365-1374 (1974).

[23] Reisberg, J. and T. Doscher: *"Interfacial Phenomena in Crude/Oil/Water Systems,"* Producer Monthly, 21, 43-50 (1956).

[24] Leach, R.O. and R.O. Wagner: *"Improving Oil Displacement Efficiency by Wettability Adjustment,"* Trans. AIME, 216, 65-72 (1959).

[25] Davies, J.T. and E.K. Rideal: *" Interfacial Phenomena,"* 2nd Edition, New York, San Francisco, and London (1963).

[26] Bansal, V.K.: *" The Effect of Caustic Concentration on Interfacial Charge, Interfacial Tension and Droplet Size, A Simple Test for Optimum Caustic Concentration for Crude Oils,"* JCPT., 17(1), 69-72 (1978).

[27] Cratin, P.D.: *" A Quantitative Characterization of pH-dependent System,"* Monograph Series, ACS, Washington D.C., 37-47 (1971).

[28] Bansal, V.K., K.S. Chan, R. McCallough, D.O. Shah: *"Effect of Caustic Concentration on Interfacial Charge, Interfacial Tension, and Droplet size,"* JCPT, 17(1), 69-72 (1978).

[29] Chan, M. and T.F. Yen: *"Role of Sodium Hydroxide in the Lowering of Interfacial Tension between Crude Oil and Alkaline Aqueous Solution,"* Fuel, 60, 552-53 (1981).

[30] Neale, G.H., K.C. Khulbe and V. Hornof: *" Effects of Oil Phase Viscosity on Interfacial Tension Behavior of Oil/Alkaline Systems as Measured by the Spinning Drop Tensiometer,"* Can. J. Chem. Eng., 62, 700-705 (1985).

[31] Neumann, H.J.: *"Interfacial Tension of Crude Oils,"* Erdol und Kohle, 17, 19-26 (1964).

[32] Nasr-El-Din, H.A., K.C. Khulbe, V. Hornof and G.H. Neale: *"Effect of Interfacial Reaction on the Radial Displacement of Oil by Alkaline Solutions,"* Revue l'Institut Francais du Petrole, 45, 231-244 (1990).

[33] Campbell, T.C.: *" The Role of Alkaline Chemicals in Oil Displacement Mechanism in Surface Phenomena in Enhanced Oil Recovery,"* Shah D.O.(Editor), Plenum Press, N.Y., 293-306 (1981).

[34] Nasr-El-Din, H.A., V. Hornof and G.H. Neale: Revue l'Institut Francais du Petrole, 42, 783-796 (1987).

[35] Perkins, T.K. and O.C. Johnson: *"A Study of Immiscible Fingering in Linear Hele-Shaw Model,"* SPEJ, 9, 39-45 (1969).

[36] Touhami, Y.: *"Effect of Viscosity on Dynamic Interfacial Tension,"* M.A.Sc Thesis, U. of Ottawa, Chemical Engineering Dept., Canada (1990).

[37] Mingzhe, T., L. Pu, Z. Lufang and Z. Yajie: *" An Improved Model for Interfacial Activity of Acidic Oil/Caustic System for Alkaline Flooding,"* Soc.Pet.Eng. 14855, 189-192 (1986).

[38] Peru, D.A. and P.B Lorenz: *" Surfactant-Enhanced Low-pH Alkaline Flooding,"* SPERE, 5, 327-332 (1990).

[39] Homsy, G.M.: "*Viscous Fingering in Porous Media,*" Ann. Rev. Fluid Mech., 19, 271-311 (1987).

Chapter 6

Appendix A

6.1 Recovery Percentage Data

Recovery percentage data for the system of 2.5 mM sodium hydroxide solution displacing paraffin oil containing 10 mM linoleic acid.

flowrate	breakthrcugh time	recovery percentage	no. of fingers
ml/h	seconds	%	
0.78	7534	9.056	3

flowrate	breakthrough time	recovery percentage	no. of fingers
ml/h	seconds	%	
3.3	2200	11.199	14

flowrate	breakthrough time	recovery percentage	no. of fingers
ml/h	seconds	%	
5.5	1100	9.33	17

Recovery percentage data for the system of 12.5 mM sodium hydroxide solution displacing paraffin oil containing 10 mM linoleic acid.

flowrate	breakthrough time	recovery percentage	no. of fingers
ml/h	seconds	%	
0.78	31500	37.9	2

flowrate	breakthrough time	recovery percentage	no. of fingers
ml/h	seconds	%	
3.3	4848	24.68	9

flowrate	breakthrough time	recovery percentage	no. of fingers
ml/h	seconds	%	
5.5	2450	20.78	13

Recovery percentage data for the system of 25 mM sodium hydroxide solution displacing paraffin oil containing 10 mM linoleic acid.

flowrate	breakthrough time	recovery percentage	no. of fingers
ml/h	seconds	%	
0.78	40000	48.129	3

flowrate	breakthrough time	recovery percentage	no. of fingers
ml/h	seconds	%	
3.3	7200	36.653	9

flowrate	breakthrough time	recovery percentage	no. of fingers
ml/h	seconds	%	
5.5	3390	28.761	16

6.2 Recovery Percentage Calculation

Recovery percentage calculation for the system of 25 mM sodium hydroxide solution displacing paraffin oil containing 10 mM linoleic acid. Flowrate was 0.78 ml/h.

$$\%Rec = \frac{Qt_{br}}{\varepsilon h \pi r^2} \times 100 \tag{6.1}$$

$$\%Rec = \frac{0.78 \times 40000}{0.39 \times 0.3 \times 3.14 \times 7^2 \times 3600} \times 100 \tag{6.2}$$

$$\%Rec = 48.128\% \tag{6.3}$$

Recovery percentage calculation for the system of 25 mM sodium hydroxide solution displacing paraffin oil containing 10 mM linoleic acid. Flowrate was 3.3 ml/h.

$$\%Rec = \frac{3.3 \times 7200}{0.39 \times 0.3 \times 3.14 \times 7^2 \times 3600} \times 100 \tag{6.4}$$

$$\%Rec = 36.65\% \tag{6.5}$$

Recovery percentage calculation for the system of 25 mM sodium hydroxide solution displacing paraffin oil containing 10 mM linoleic acid. Flowrate was 5.5 ml/h.

$$\%Rec = \frac{5.5 \times 3390.0}{0.39 \times 0.3 \times 3.14 \times 7^2 \times 3600} \times 100 \tag{6.6}$$

$$\%Rec = 28.761\% \tag{6.7}$$